Supporting Information

Identifying Effects of Phosphorous in Transition Metal Phosphides for Selective Hydrogenolysis of Hindered C–O Bonds

Conor Waldt,[1] Hansel Montalvo-Castro,[1] Abdulrahman Almithn,[1,2] Álvaro Loaiza-Orduz,[3] Craig Plaisance,[3] David Hibbitts[1]*

[1]*Department of Chemical Engineering, University of Florida, Gainesville, FL 32608, USA*

[2]*Department of Chemical Engineering, King Faisal University, Al Hofuf, Eastern Province 31982, Saudi Arabia*

[3]*Cain Department of Chemical Engineering, Louisiana State University, Baton Rouge, Louisiana 70803, USA*

*Corresponding author: hibbitts@che.ufl.edu

Table of Contents

S1. *DFT Calculations*

S1.1 *Bulk Lattice Parameters and Surface Formation*

Energy convergence tests were performed for all materials (Figure S1). For the M_2P materials k-point meshes of 4 × 4 × 7, 12 × 12 × 21, and 20 × 20 × 35 were used. Change in energy from the 12 × 12 × 21 meshes to 20 × 20 × 35 meshes were less than 1×10^{-3}. For the FCC pure metals, meshes of 5 × 5 × 5, 7 × 7 × 7, 9 × 9 × 9, and 12 × 12 × 12 were used and changes in energy were less than 1×10^{-2} moving towards the largest mesh. For the HCP pure metals, meshes of 3 × 3 × 2, 6 × 6 × 4, 9 × 9 × 6, and 12 × 12 × 9 were used with changes in energy being less than 5×10^{-3} when approaching the largest mesh. The largest mesh for each material was cleaved to form surfaces.

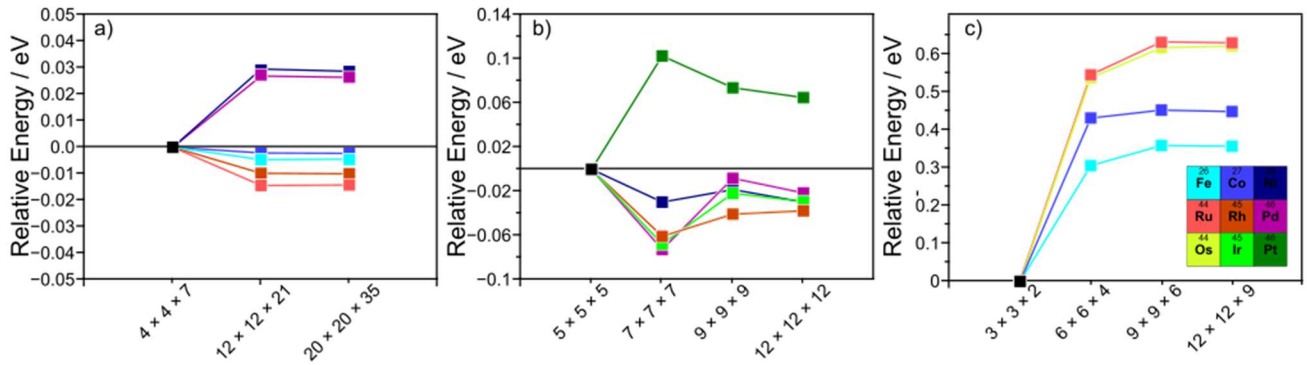

Figure S1. K-point convergence test for all M_2P (a), pure FCC metal (b), and pure HCP metal (c) surfaces. The periodic table in the bottom right provides the color key.

S1.2 *Temperature Corrected Enthalpies, Entropies, and Gibbs Free Energies*

Enthalpies (H) and Gibb's free energies (G) can be calculated from density functional theory (DFT)-derived energies using statistical mechanics. Specifically, each is a sum of the electronic energy (E_0), the zero-point vibrational energy (ZPVE), and the respective vibrational, translational, and rotational motions of the species:

$$H = E_o + ZPVE + H_{vib} + H_{rot} + H_{trans} \quad \text{(S1)}$$

$$G = E_0 + ZPVE + G_{vib} + G_{rot} + G_{trans} \quad \text{(S2)}$$

at 523 K. Adsorbed species are not considered to have translational or rotational contributions; all such motions are modeled as frustrated vibrations on the metal and metal phosphide surfaces. Vibrational, rotational, and translational enthalpies and free energies are estimated from other statistical mechanics formalisms:

$$ZPVE = \sum_i \left(\frac{1}{2} h\nu_i\right) \quad \text{(S3)}$$

$$H_{vib} = \sum_i \left(\frac{h\nu_i \exp\left(-\frac{h\nu_i}{kT}\right)}{1-\exp\left(-\frac{h\nu_i}{kT}\right)}\right) \quad \text{(S4)}$$

$$G_{vib} = \sum_i \left(-kT \ln\left(\frac{1}{1-\exp\left(-\frac{h\nu_i}{kT}\right)}\right)\right) \quad \text{(S5)}$$

$$H_{trans} = \frac{5}{2} kT \quad \text{(S6)}$$

$$H_{rot,linear} = kT \quad \text{(S7)}$$

$$H_{rot,nonlinear} = \frac{3}{2} kT \quad \text{(S8)}$$

$$G_{trans} = -kT \ln\left(\left(\frac{2\pi mkT}{h^2}\right)^{\frac{3}{2}} V\right) \tag{S9}$$

$$G_{rot} = -kT \ln\left(\frac{\pi^{\frac{1}{2}}}{\sigma}\left(\frac{T^3}{\theta_x\theta_y\theta_z}\right)^{\frac{1}{2}}\right) \tag{S10}$$

$$\theta_i = \frac{h^2}{8\pi^2 I_i k} \tag{S11}$$

where I_i is the moment of intertia about the i axis (either x, y, or z) and σ is the symmetry number of the species.[1]

S2. ***Bulk Material Restructuring***

During the bulk parameter optimization, three of the M_2P models restructured significantly, warranting their exclusion from the rest of the study. These materials were Pt_2P, Ir_2P, and Os_2P. Pt_2P and Ir_2P visibly restructure to form a more hexagonal shape (Figure S1). Os_2P also significantly restructures, though this may not be as clearly visible in Figure S1, but the bulk formation energy for Os_2P is very poor in comparison to Ni_2P.

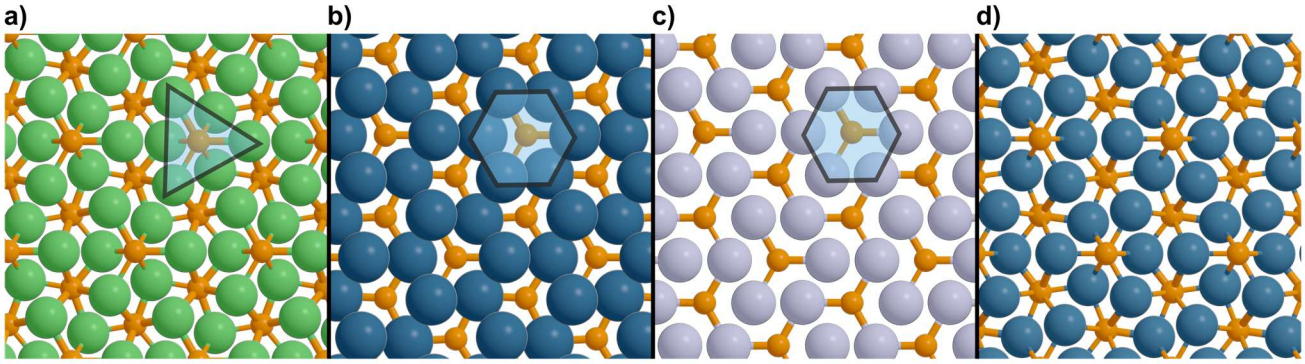

Figure S2. Bulk material structures for Ni_2P (a), Ir_2P (b), Pt_2P (c), and Os_2P (d). Highlighted are the general structure of the metal atoms coordinated with a single P atom.

S3. *Reaction Coordinate Diagrams*

The reaction coordinate diagrams for Fe(0001) and Fe_2P(001) (Figure S3), Rh(111) and Rh_2P(001) (Figure S4), Ru(0001) and Ru_2P (Figure S5), Pt(111) (Figure S6), and Ir(111) (Figure S7) all indicate that these materials activated both the ^{2}C–O and ^{3}C–O bonds via similar mechanisms as that reported for Ni(111) and Ni_2P(001). In all cases the relative enthalpy barrier (in reference to the bare surface and gas phase MTHF and H_2) for C–H activation is lower than that for the correspond C–O activation at the same reaction coordinate. Also, in almost every case, the free energy barrier for the fully dehydrogenated C–O activation is the most favorable.

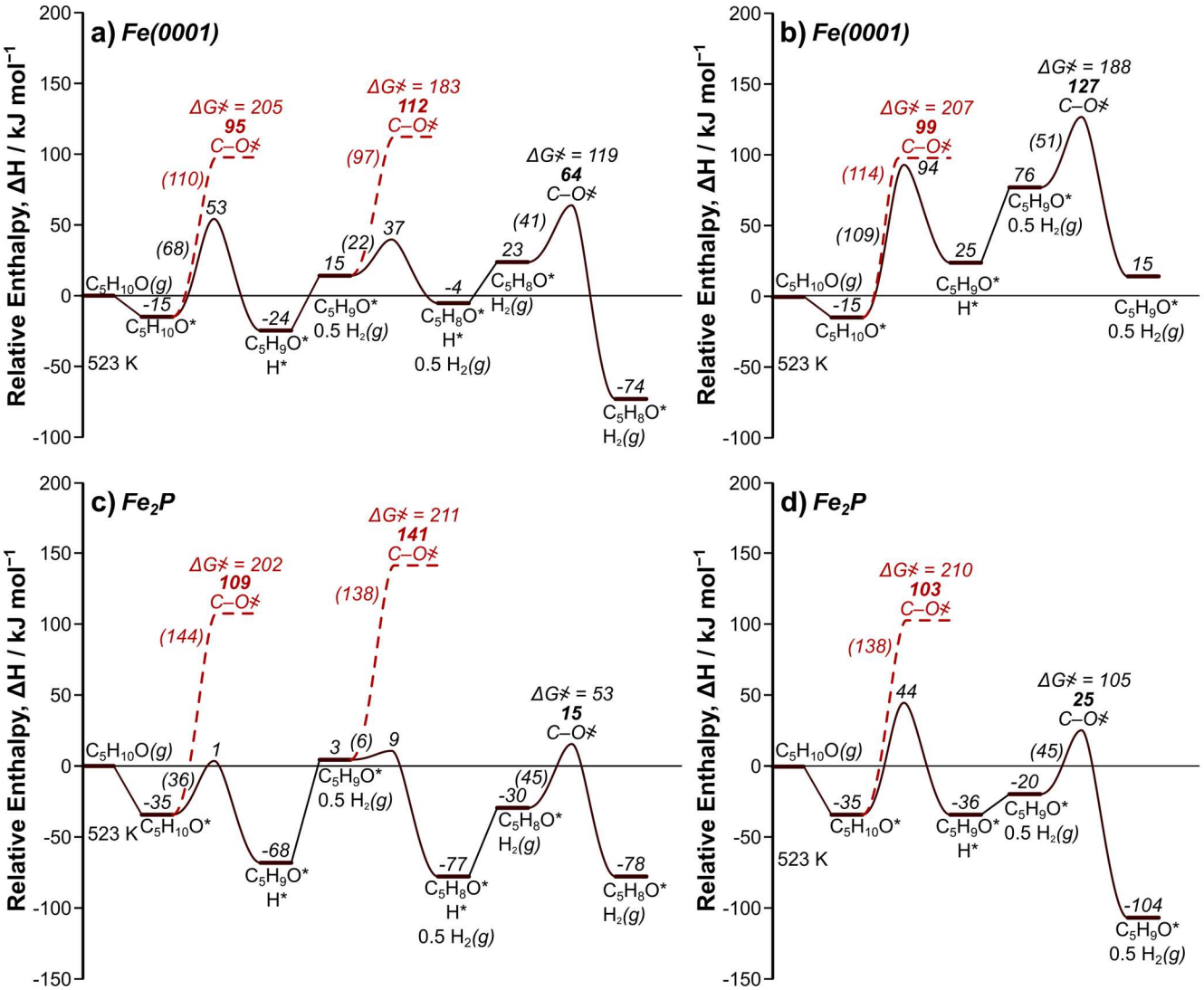

Figure S3. Reaction coordinate diagrams relative to the bare surface and gas phase MTHF at 523 K for Fe(0001) for the ^{2}C–O bond activation (a) and the ^{3}C–O bond activation (b) along with the reaction coordinate diagrams for Fe_2P(001) for the ^{2}C–O bond activation (c) and the ^{3}C–O bond activation (d). The solid black lines indicate the main (fully dehydrogenated) reaction pathway. The dashed red lines indicate alternate pathways where a C–O bond is activated before full dehydrogenation. The red and black numbers correspond to the relative enthalpies of their respective reactant, product, or transition state. The intrinsic activation barriers (ΔH_{act}) are provided in parentheses for each reaction step.

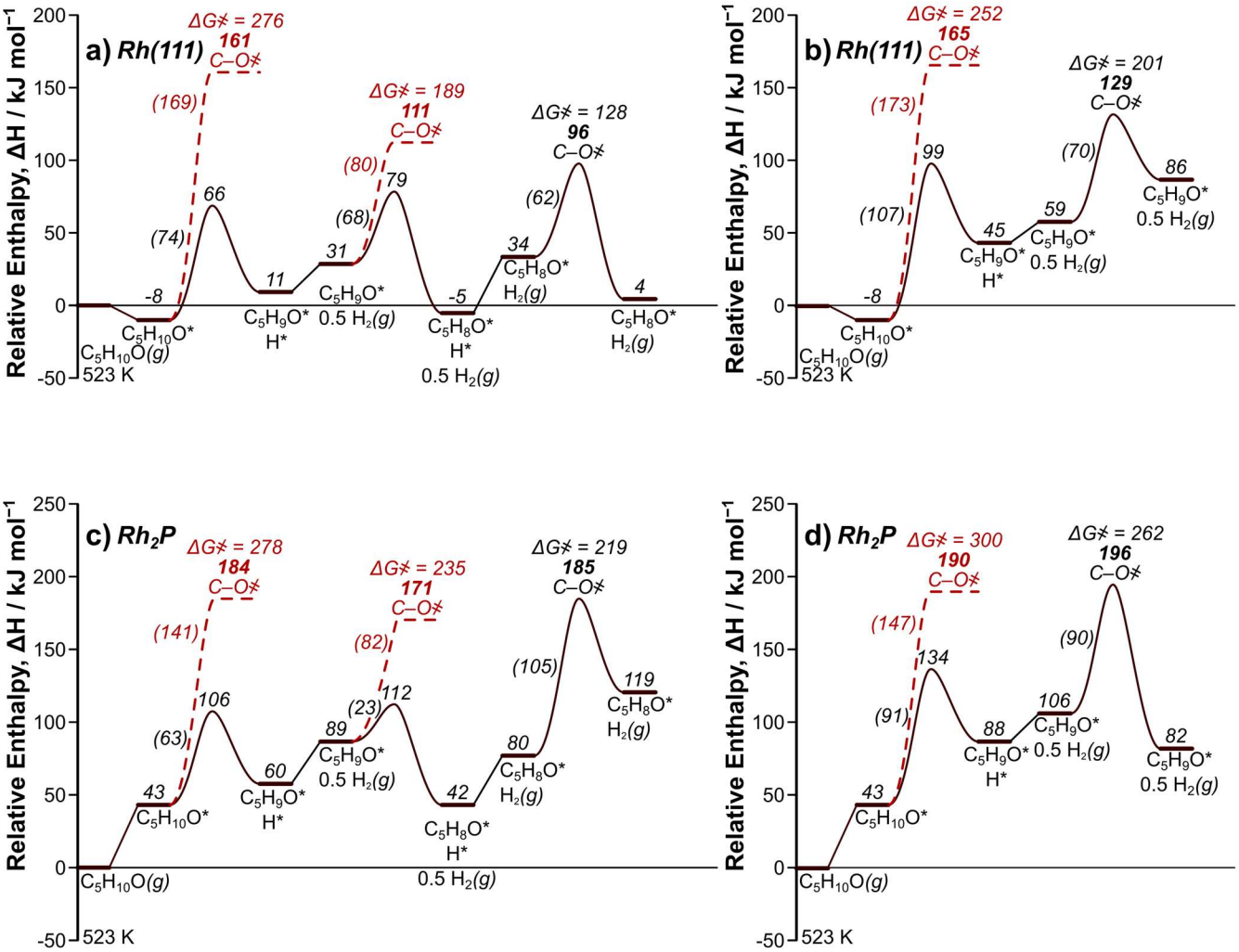

Figure S4. Reaction coordinate diagrams relative to the bare surface and gas phase MTHF at 523 K for Rh(111) for the ^{2}C–O bond activation (a) and the ^{3}C–O bond activation (b) along with the reaction coordinate diagrams for $Rh_2P(001)$ for the ^{2}C–O bond activation (c) and the ^{3}C–O bond activation (d). The solid black lines indicate the main (fully dehydrogenated) reaction pathway. The dashed red lines indicate alternate pathways where a C–O bond is activated before full dehydrogenation. The red and black numbers correspond to the relative enthalpies of their respective reactant, product, or transition state. The intrinsic activation barriers (ΔH_{act}) are provided in parentheses for each reaction step.

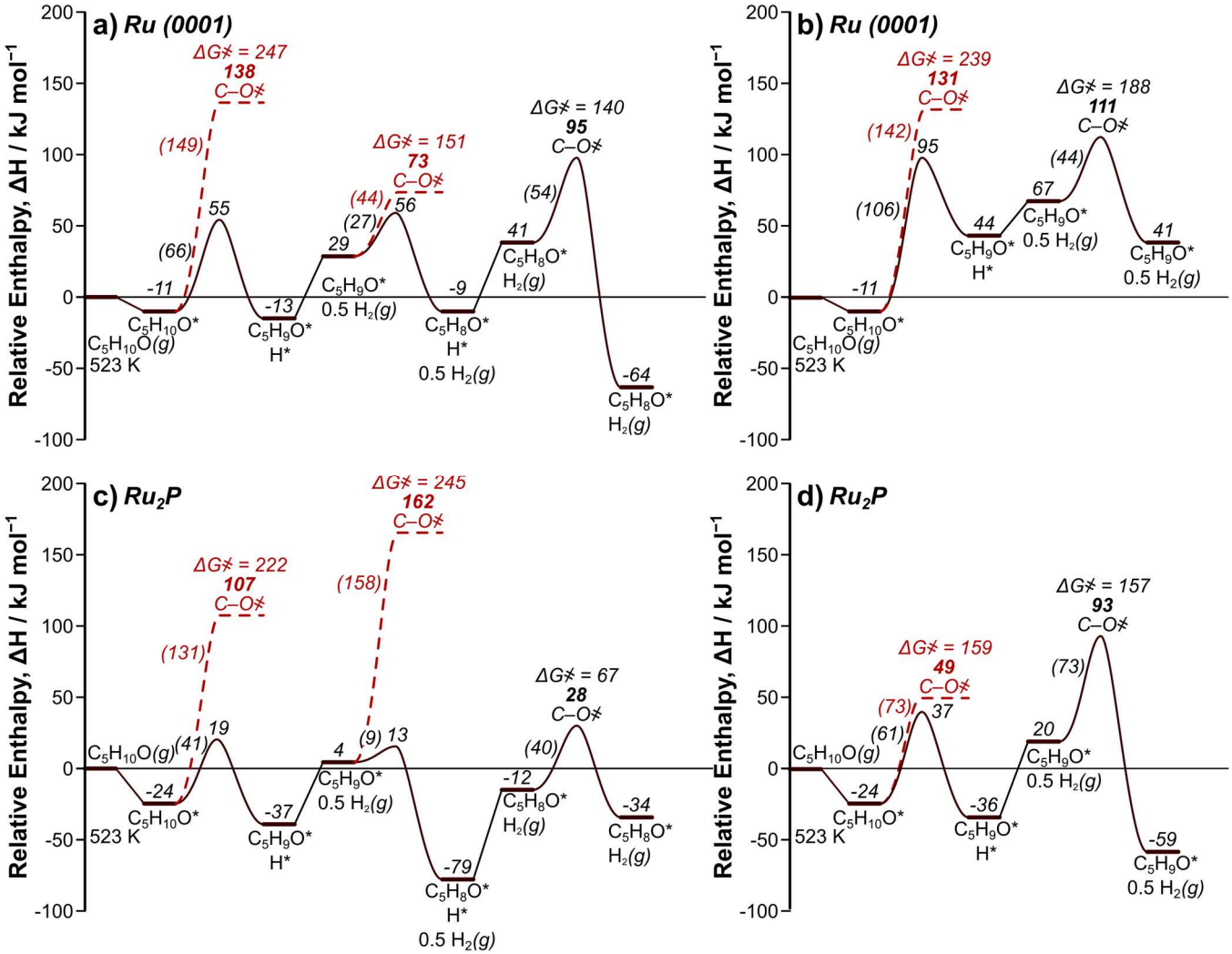

Figure S5. Reaction coordinate diagrams relative to the bare surface and gas phase MTHF at 523 K for Ru(0001) for the ^{2}C–O bond activation (a) and the ^{3}C–O bond activation (b) along with the reaction coordinate diagrams for Ru_2P(001) for the ^{2}C–O bond activation (c) and the ^{3}C–O bond activation (d). The solid black lines indicate the main (fully dehydrogenated) reaction pathway. The dashed red lines indicate alternate pathways where a C–O bond is activated before full dehydrogenation. The red and black numbers correspond to the relative enthalpies of their respective reactant, product, or transition state. The intrinsic activation barriers (ΔH_{act}) are provided in parentheses for each reaction step.

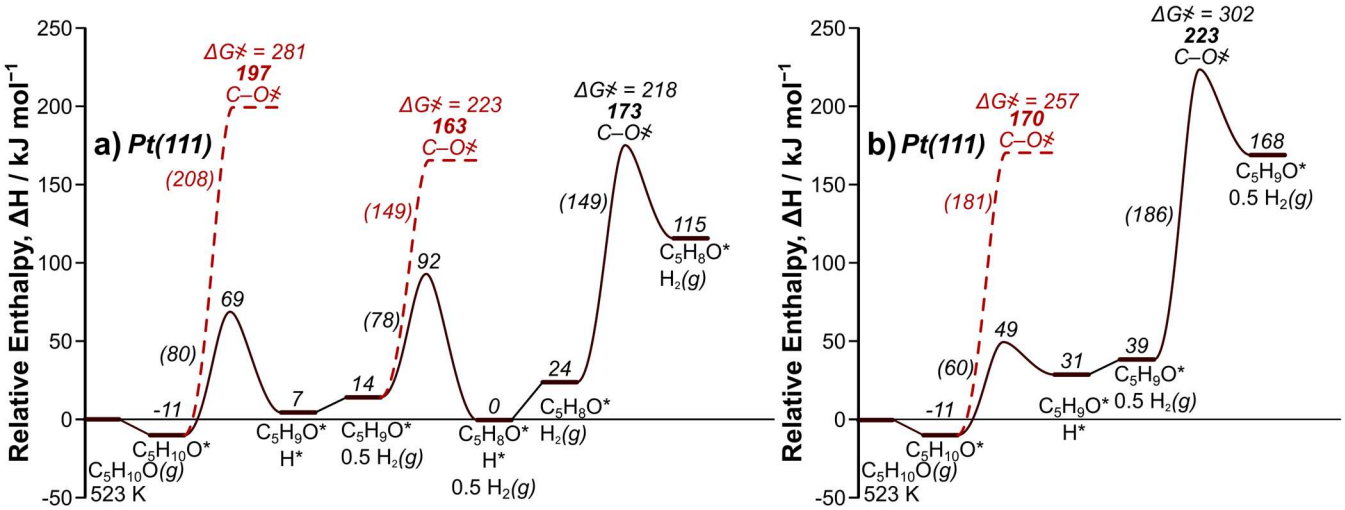

Figure S6. Reaction coordinate diagrams relative to the bare surface and gas phase MTHF at 523 K for Pt(111) for the ^{2}C–O bond activation (a) and the ^{3}C–O bond activation (b). The solid black lines indicate the main (fully dehydrogenated) reaction pathway. The dashed red lines indicate alternate pathways where a C–O bond is activated before full dehydrogenation. The red and black numbers correspond to the relative enthalpies of their respective reactant, product, or transition state. The intrinsic activation barriers (ΔH_{act}) are provided in parentheses for each reaction step.

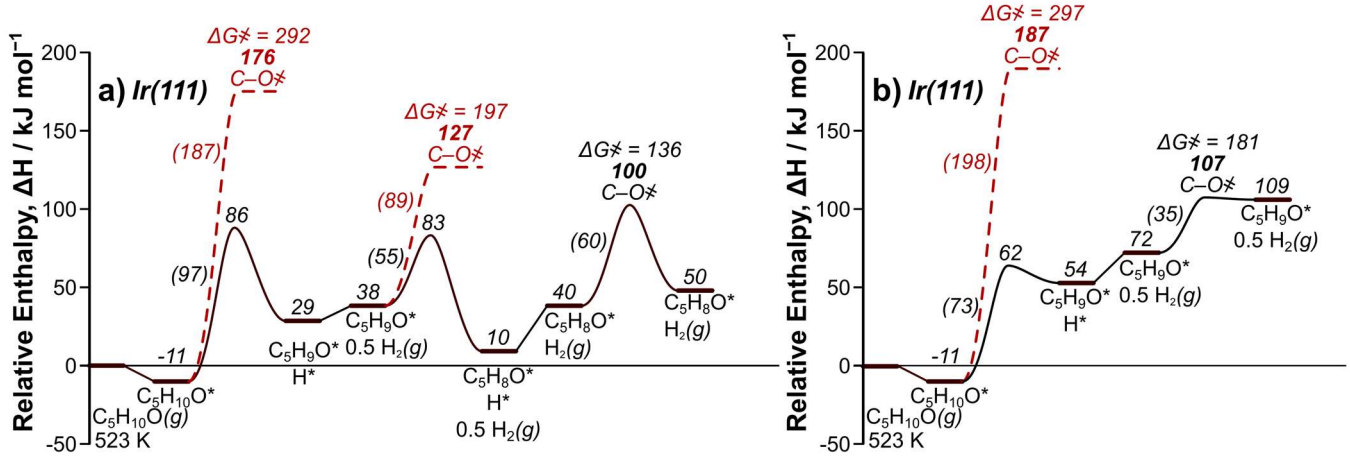

Figure S7. Reaction coordinate diagrams relative to the bare surface and gas phase MTHF at 523 K for Ir(111) for the ^{2}C–O bond activation (a) and the ^{3}C–O bond activation (b). The solid black lines indicate the main (fully dehydrogenated) reaction pathway. The dashed red lines indicate alternate pathways where a C–O bond is activated before full dehydrogenation. The red and black numbers correspond to the relative enthalpies of their respective reactant, product, or transition state. The intrinsic activation barriers (ΔH_{act}) are provided in parentheses for each reaction step.

S4. *Structure Images, Enthalpies, Entropies, and Free Energies for All Reaction States*

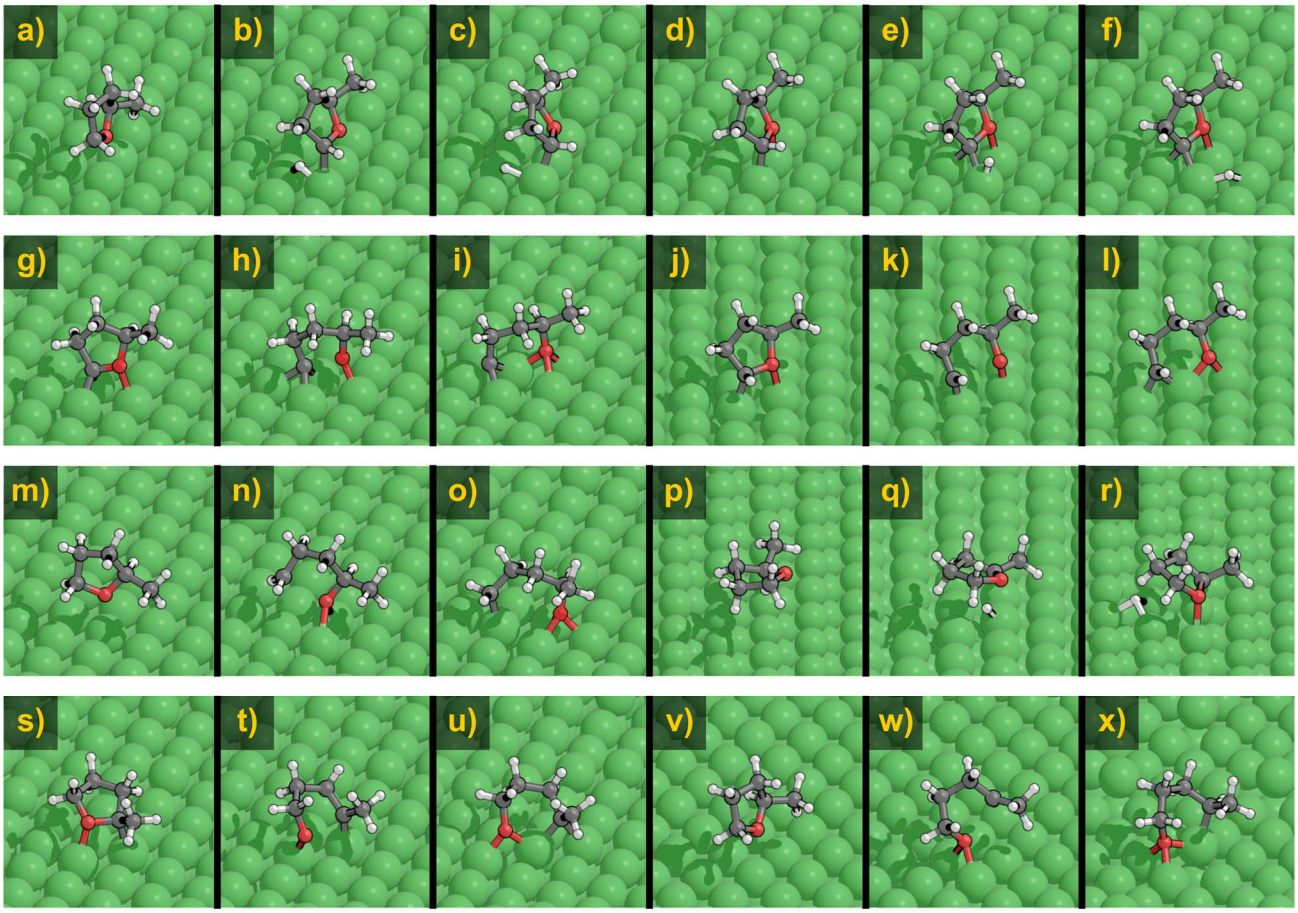

Figure S8. Structural images for the complete pathways for both the ^{2}C–O (a–i) and ^{3}C–O (p–u) activations along with the alternate C–O activations (j–o, v–x) over a Ni(111) surface.

Table S1. Enthalpies (kJ mol^{-1}), entropies (J mol^{-1}), and free energies (kJ mol^{-1}) for the ^{2}C–O activation of MTHF over a Ni(111) surface (543 K). These states correspond to the reaction coordinate diagram in Figure 2a.

		$C_5H_{10}O \rightarrow C_5H_9O$			$C_5H_9O \rightarrow C_5H_8O$			$C_5H_8O \rightarrow C_5H_8O$			$C_5H_9O \rightarrow C_5H_9O$			$C_5H_{10}O \rightarrow C_5H_{10}O$		
Rxn Step	BS[a]	R	TS	P	R	TS	P	R	TS	P	R	TS	P	R	TS	P
ΔH	0	15	85	57	66	95	30	68	133	32	66	157	78	15	170	28
ΔS	0	−251	−222	−194	−164	−141	−97	−68	−56	−63	−131	−123	−143	−247	−171	−203
ΔG	0	130	192	149	143	163	74	99	163	64	132	224	153	129	263	134
Figure	N/A	S8a	S8b	S8c	S8d	S8e	S8f	S8g	S8h	S8i	S8j	S8k	S8l	S8m	S8n	S8o

[a]Overall values for the bare surface (BS)

Table S2. Enthalpies (kJ mol^{-1}), entropies (J mol^{-1}), and free energies (kJ mol^{-1}) for the ^{3}C–O activation of MTHF over a Ni(111) surface (523 K). These states correspond to the reaction coordinate diagram in Figure 2b.

	$C_5H_{10}O \rightarrow C_5H_9O$	$C_5H_9O \rightarrow C_5H_9O$	$C_5H_{10}O \rightarrow C_5H_{10}O$

Rxn Coord.	BS[a]	R	TS	P	R	TS	P	R	TS	P
ΔH	0	15	90	75	97	181	113	−2	137	74
ΔS	0	−243	−164	−211	−143	−103	−117	−249	−168	−196
ΔG	0	118	179	175	167	237	184	128	228	176
Figure	N/A	S8p	S8q	S8r	S8s	S8t	S8u	S8v	S8w	S8x

[a]Overall values for the bare surface (BS)

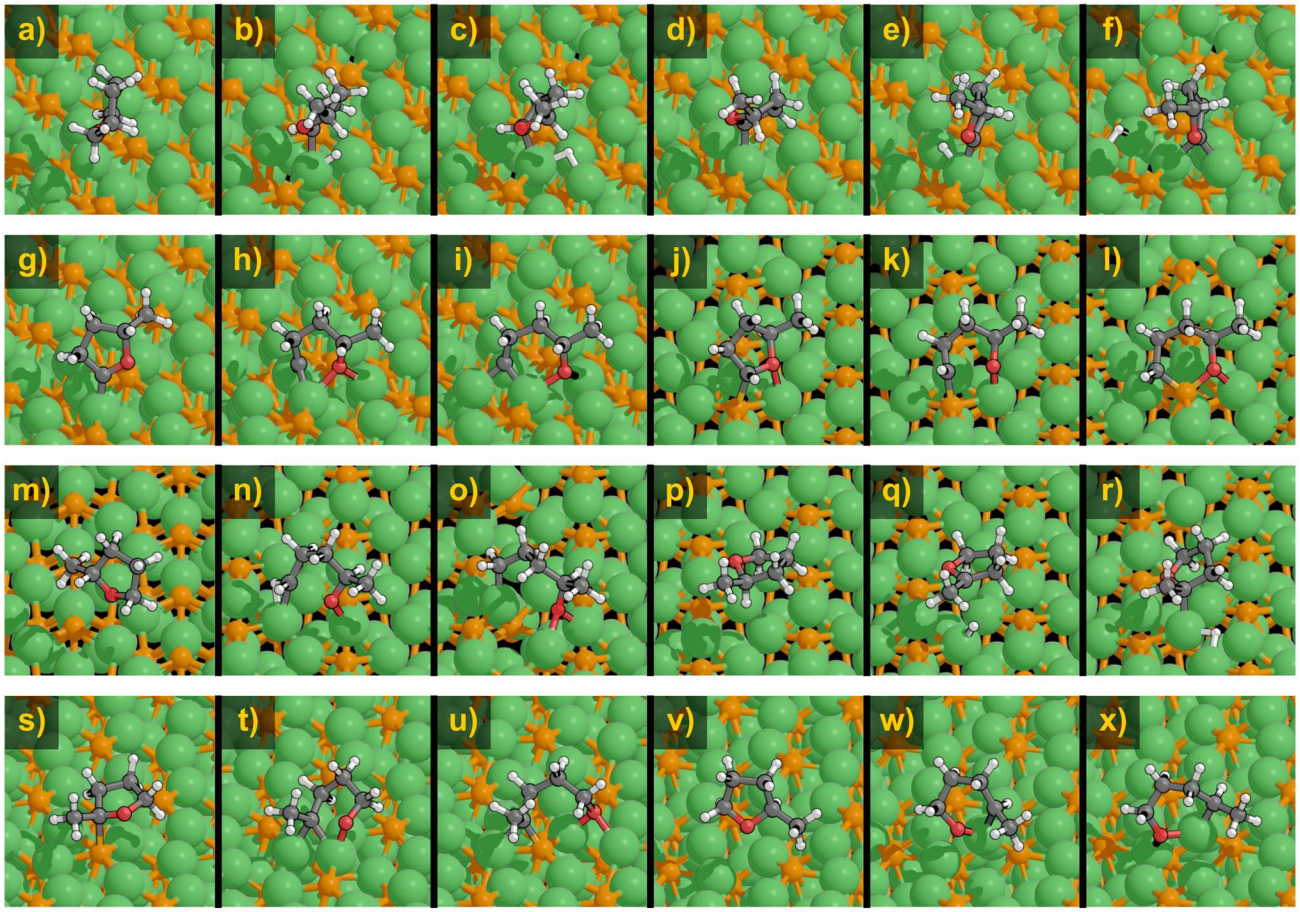

Figure S9. Structural images for the complete pathways for both the ^{2}C–O (a–i) and ^{3}C–O (p–u) activations along with the alternate C–O activations (j–o, v–x) over a $Ni_2P(001)$ surface.

Table S3. Enthalpies (kJ mol^{-1}), entropies (J mol^{-1}), and free energies (kJ mol^{-1}) for the ^{2}C–O activation of MTHF over a $Ni_2P(001)$ surface (543 K). These states correspond to the reaction coordinate diagram in Figure 2c.

		$C_5H_{10}O \rightarrow C_5H_9O$			$C_5H_9O \rightarrow C_5H_8O$			$C_5H_8O \rightarrow C_5H_8O$			$C_5H_9O \rightarrow C_5H_9O$			$C_5H_{10}O \rightarrow C_5H_{10}O$		
Rxn Step	BS[a]	R	TS	P	R	TS	P	R	TS	P	R	TS	P	R	TS	P
ΔH	0	4	89	85	57	128	94	97	182	76	57	162	90	4	144	60
ΔS	0	−186	−220	−216	−144	−165	−104	−61	−71	−74	−114	−135	−133	−213	−189	−180
ΔG	0	95	195	188	154	205	142	100	221	114	117	236	159	104	246	154

Figure	3b	S9a	S9b	S9c	S9d	S9e	S9f	S9g	S9h	S9i	S9j	S9k	S9l	S9m	S9n	S9o

[a]Overall values for the bare surface (BS)

Table S4. Enthalpies (kJ mol^{-1}), entropies (J mol^{-1}), and free energies (kJ mol^{-1}) for the ^{3}C–O activation of MTHF over a $Ni_2P(001)$ surface (543 K). These states correspond to the reaction coordinate diagram in Figure 2d.

		$C_5H_{10}O \rightarrow C_5H_9O$			$C_5H_9O \rightarrow C_5H_9O$			$C_5H_{10}O \rightarrow C_5H_{10}O$		
Rxn Coord.	BS[a]	R	TS	P	R	TS	P	R	TS	P
ΔH	0	4	115	106	85	148	83	4	143	76
ΔS	0	−186	−220	−216	−144	−135	−104	−70	−180	−74
ΔG	0	95	195	188	154	221	142	105	240	114
Figure	3b	S9p	S9q	S9r	S9s	S9t	S9u	S9v	S9w	S9x

[a]Overall values for the bare surface (BS)

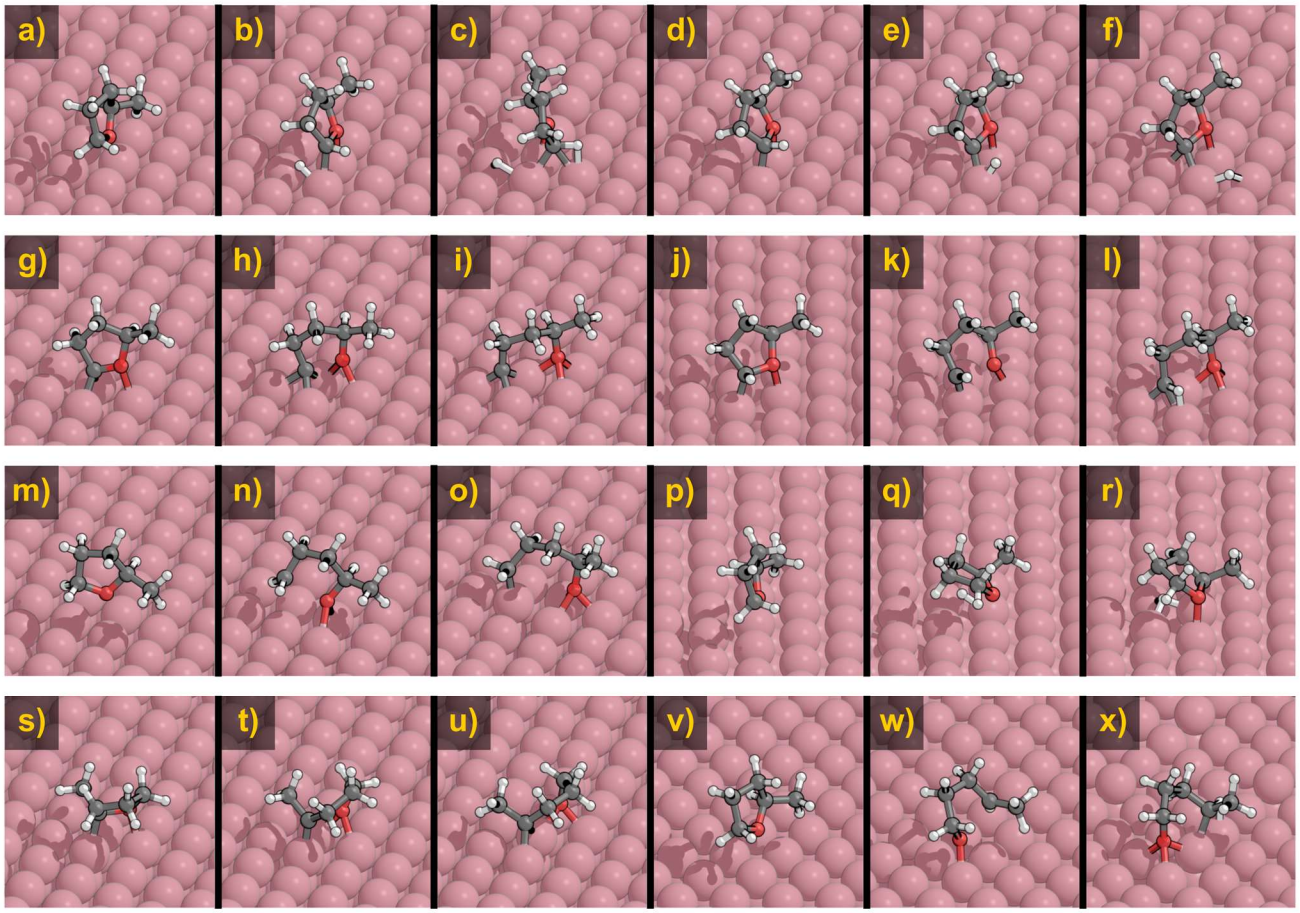

Figure S10. Structural images for the complete pathways for both the ^{2}C–O (a–i) and ^{3}C–O (p–u) activations along with the alternate C–O activations (j–o, v–x) over a Co(0001) surface.

Table S5. Enthalpies (kJ mol^{-1}), entropies (J mol^{-1}), and free energies (kJ mol^{-1}) for the ^{2}C–O activation of MTHF over a Co(0001) surface (523 K). These states correspond to the reaction coordinate diagram in Figure 4a.

		$C_5H_{10}O \rightarrow C_5H_9O$			$C_5H_9O \rightarrow C_5H_8O$			$C_5H_8O \rightarrow C_5H_8O$			$C_5H_9O \rightarrow C_5H_9O$			$C_5H_{10}O \rightarrow C_5H_{10}O$		
Rxn Step	BS[a]	R	TS	P	R	TS	P	R	TS	P	R	TS	P	R	TS	P
ΔH	0	−12	84	30	63	95	37	70	123	−6	63	147	16	−12	152	18
ΔS	0	−240	−195	−205	−162	−119	−134	−92	−77	−62	−162	−192	−151	−245	−174	−184
ΔG	0	113	186	138	148	157	107	118	163	26	148	248	95	116	243	114
Figure	N/A	S10a	S10b	S10c	S10d	S10e	S10f	S10g	S10h	S10i	S10j	S10k	S10l	S10m	S10n	S10o

[a]Overall values for the bare surface (BS)

Table S6. Enthalpies (kJ mol^{-1}), entropies (J mol^{-1}), and free energies (kJ mol^{-1}) for the ^{3}C–O activation of MTHF over a Co(0001) surface (523 K). These states correspond to the reaction coordinate diagram in Figure 4b.

		$C_5H_{10}O \rightarrow C_5H_9O$			$C_5H_9O \rightarrow C_5H_9O$			$C_5H_{10}O \rightarrow C_5H_{10}O$		
Rxn Coord.	BS[a]	R	TS	P	R	TS	P	R	TS	P
ΔH	0	−13	116	85	97	159	87	−10	140	35
ΔS	0	−238	−227	−210	−158	−132	−148	−252	−231	−209
ΔG	0	112	235	195	180	228	164	122	261	144
Figure	N/A	S10p	S10q	S10r	S10s	S10t	S10u	S10v	S10w	S10x

[a]Overall values for the bare surface (BS)

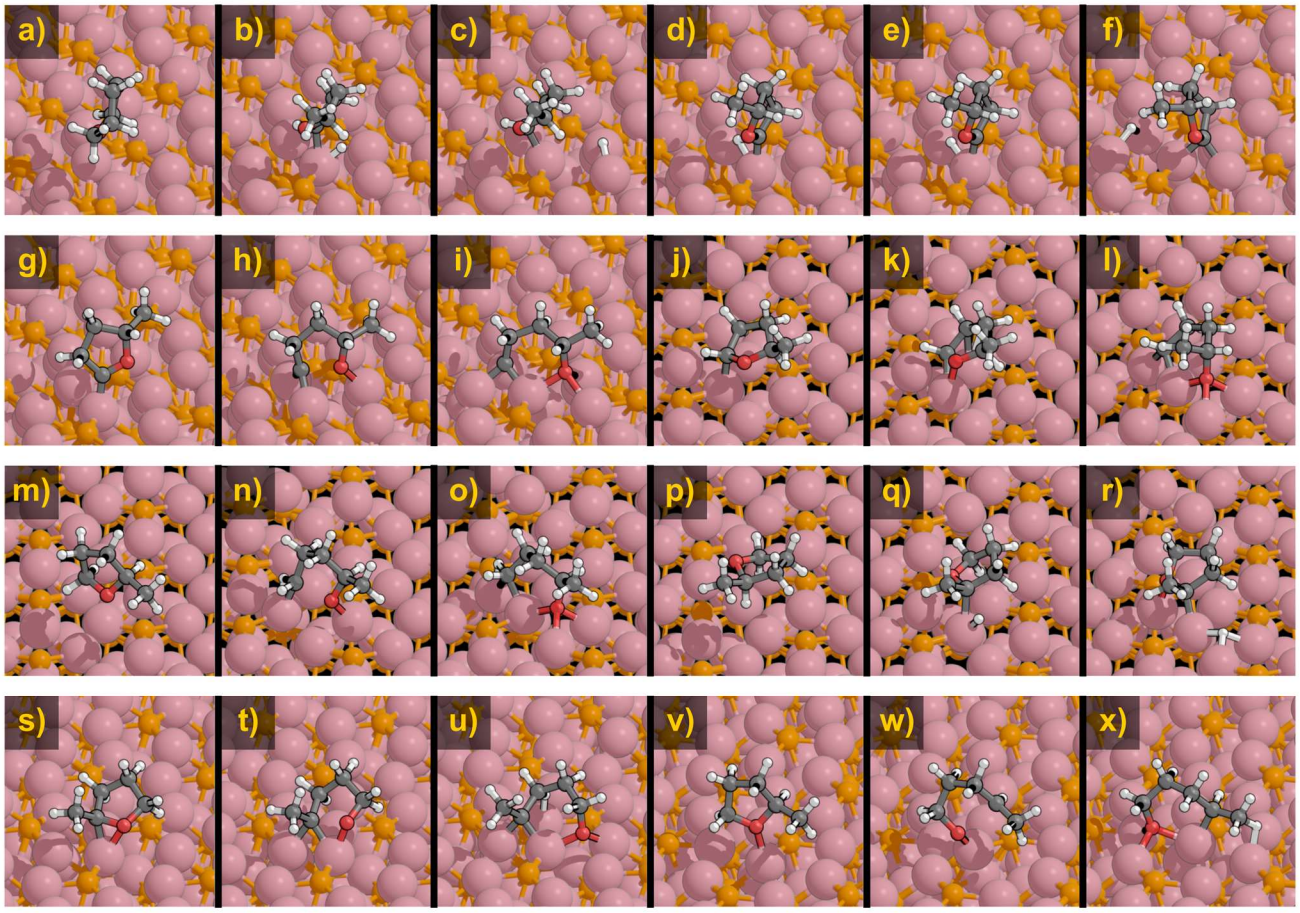

Figure S11. Structural images for the complete pathways for both the ^{2}C–O (a−i) and ^{3}C–O (p−u) activations along with the alternate C–O activations (j−o, v−x) over a $Co_2P(001)$ surface.

Table S7. Enthalpies (kJ mol^{-1}), entropies (J mol^{-1}), and free energies (kJ mol^{-1}) for the ^{2}C–O activation of MTHF over a $Co_2P(001)$ surface (523 K). These states correspond to the reaction coordinate diagram in Figure 4c.

		$C_5H_{10}O \rightarrow C_5H_9O$			$C_5H_9O \rightarrow C_5H_8O$			$C_5H_8O \rightarrow C_5H_8O$			$C_5H_9O \rightarrow C_5H_9O$			$C_5H_{10}O \rightarrow C_5H_{10}O$		
Rxn Step	BS[a]	R	TS	P	R	TS	P	R	TS	P	R	TS	P	R	TS	P
ΔH	0	−6	79	25	39	45	−9	21	76	−95	55	100	−27	−6	86	−57
ΔS	0	−209	−93	−185	−177	−141	−96	−66	−67	−76	−101	−160	−127	−192	−218	−191
ΔG	0	104	128	122	131	119	41	55	111	−55	108	184	39	94	200	43
Figure	3f	S11a	S11b	S11c	S11d	S11e	S11f	S11g	S11h	S11i	S11j	S11k	S11l	S11m	S11n	S11o

[a]Overall values for the bare surface (BS)

Table S8. Enthalpies (kJ mol^{-1}), entropies (J mol^{-1}), and free energies (kJ mol^{-1}) for the ^{3}C–O activation of MTHF over a $Co_2P(001)$ surface (523 K). These states correspond to the reaction coordinate diagram in Figure 4d.

		$C_5H_{10}O \rightarrow C_5H_9O$			$C_5H_9O \rightarrow C_5H_9O$			$C_5H_{10}O \rightarrow C_5H_{10}O$		
Rxn Coord.	BS[a]	R	TS	P	R	TS	P	R	TS	P

ΔH	0	−10	84	23	69	95	−16	−25	110	−10
ΔS	0	−207	−179	−193	−115	−135	−135	−215	−187	−197
ΔG	0	98	178	124	129	165	54	87	207	93
Figure	3f	S11p	S11q	S11r	S11s	S11t	S11u	S11v	S11w	S11x

[a]Overall values for the bare surface (BS)

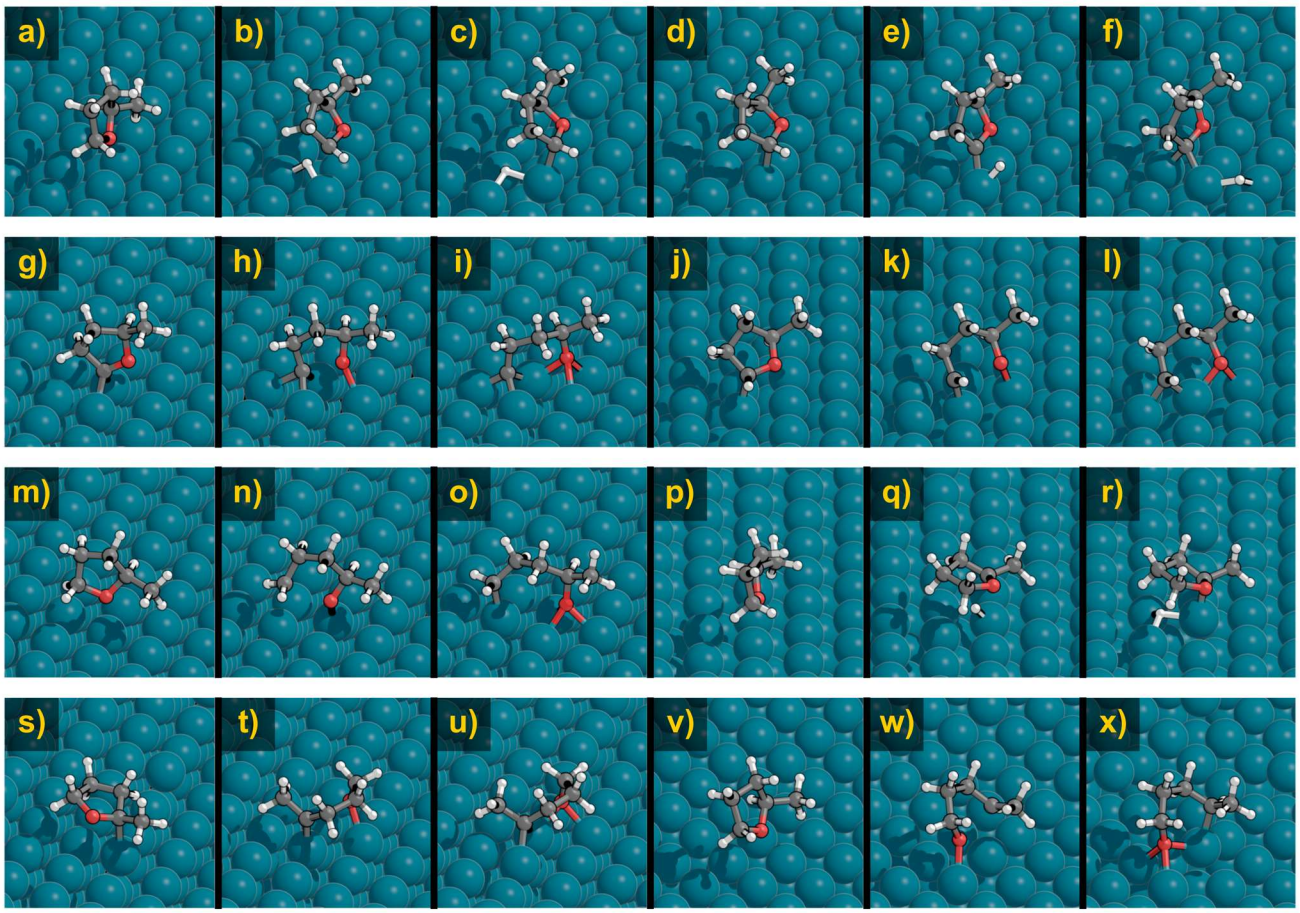

Figure S12. Structural images for the complete pathways for both the ^{2}C–O (a–i) and ^{3}C–O (p–u) activations along with the alternate C–O activations (j–o, v–x) over a Pd(111) surface.

Table S9. Enthalpies (kJ mol^{-1}), entropies (J mol^{-1}), and free energies (kJ mol^{-1}) for the ^{2}C–O activation of MTHF over a Pd(111) surface (523 K). These states correspond to the reaction coordinate diagram in Figure 6a.

		$C_5H_{10}O \rightarrow C_5H_9O$			$C_5H_9O \rightarrow C_5H_8O$			$C_5H_8O \rightarrow C_5H_8O$			$C_5H_9O \rightarrow C_5H_9O$			$C_5H_{10}O \rightarrow C_5H_{10}O$		
Rxn Step	BS[a]	R	TS	P	R	TS	P	R	TS	P	R	TS	P	R	TS	P
ΔH	0	−9	79	9	30	136	8	39	168	99	38	182	125	4	199	90
ΔS	0	−240	−186	−217	−146	−121	−124	−72	−78	−59	−125	−146	−120	−212	−175	−199
ΔG	0	117	176	122	106	200	73	76	209	130	103	259	188	115	291	194
Figure	N/A	S12a	S12b	S12c	S12d	S12e	S12f	S12g	S12h	S12i	S12j	S12k	S12l	S12m	S12n	S12o

[a]Overall values for the bare surface (BS)

Table S10. Enthalpies (kJ mol^{-1}), entropies (J mol^{-1}), and free energies (kJ mol^{-1}) for the ^{3}C–O activation of MTHF over a Pd(111) surface (523 K). These states correspond to the reaction coordinate diagram in Figure 6b.

		$C_5H_{10}O \rightarrow C_5H_9O$			$C_5H_9O \rightarrow C_5H_9O$			$C_5H_{10}O \rightarrow C_5H_{10}O$		
Rxn Coord.	BS[a]	R	TS	P	R	TS	P	R	TS	P
ΔH	0	1	78	30	58	216	157	−12	203	123
ΔS	0	−219	−198	−196	−54	−151	−146	−240	−169	−195
ΔG	0	115	181	133	86	295	233	114	292	225
Figure	N/A	S12p	S12q	S12r	S12s	S12t	S12u	S12v	S12w	S12x

[a]Overall values for the bare surface (BS)

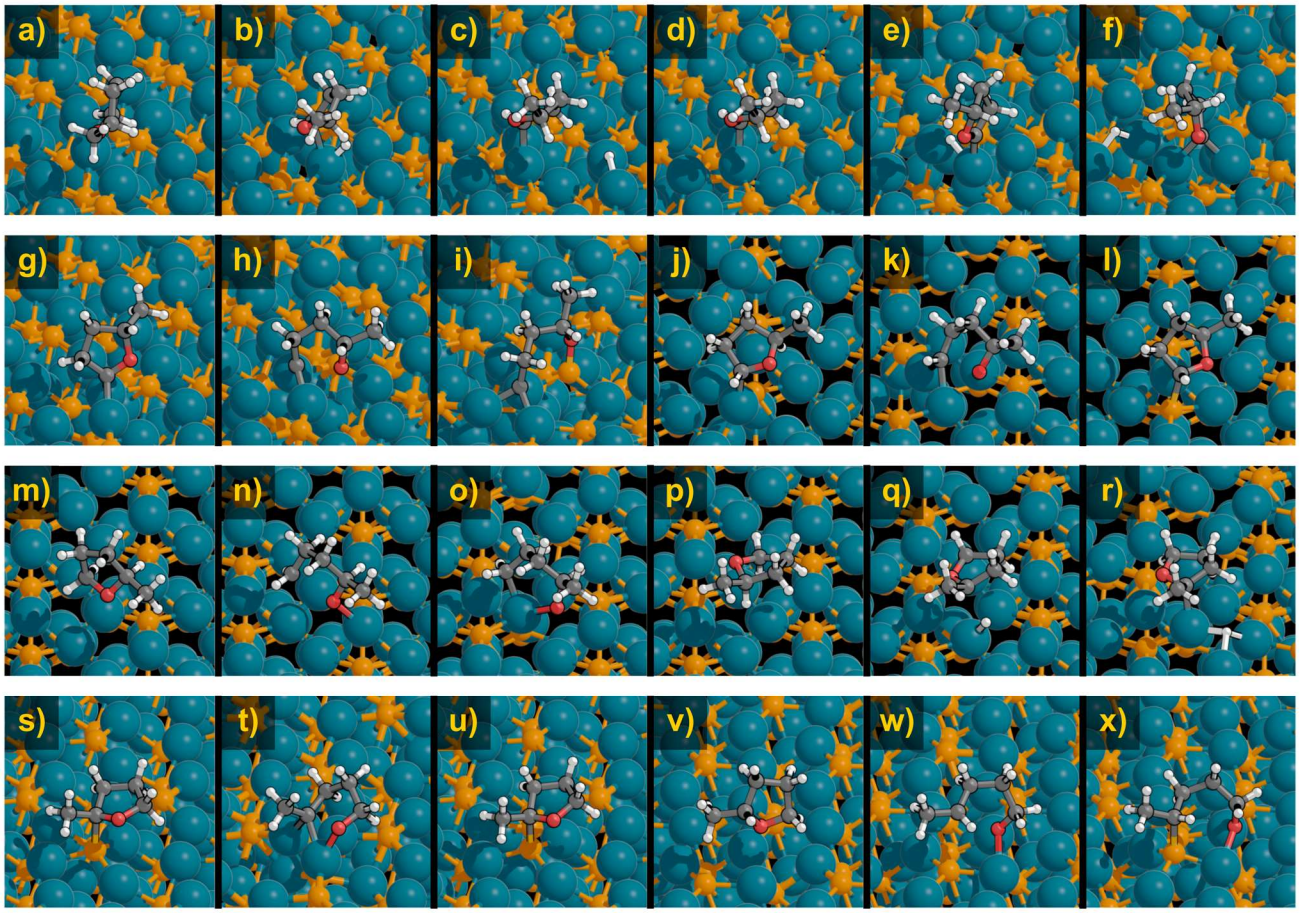

Figure S13. Structural images for the complete pathways for both the ^{2}C–O (a−i) and ^{3}C–O (p−u) activations along with the alternate C–O activations (j−o, v−x) over a $Pd_2P(001)$ surface.

Table S11. Enthalpies (kJ mol^{-1}), entropies (J mol^{-1}), and free energies (kJ mol^{-1}) for the ^{2}C–O activation of MTHF over a $Pd_2P(001)$ surface (523 K). These states correspond to the reaction coordinate diagram in Figure 6c.

		$C_5H_{10}O \rightarrow C_5H_9O$			$C_5H_9O \rightarrow C_5H_8O$			$C_5H_8O \rightarrow C_5H_8O$			$C_5H_9O \rightarrow C_5H_9O$			$C_5H_{10}O \rightarrow C_5H_{10}O$		
Rxn Step	BS[a]	R	TS	P	R	TS	P	R	TS	P	R	TS	P	R	TS	P

ΔH	0	15	146	108	89	175	136	120	292	186	−298	282	74	11	208	129
ΔS	0	−208	−191	−190	−121	−132	−134	−70	−71	−86	−341	−143	−143	−214	−190	−170
ΔG	0	124	246	207	152	244	206	157	329	231	−120	357	149	123	307	218
Figure	3n	S13a	S13b	S13c	S13d	S13e	S13f	S13g	S13h	S13i	S13j	S13k	S13l	S13m	S13n	S13o

[a]Overall values for the bare surface (BS)

Table S12. Enthalpies (kJ mol^{-1}), entropies (J mol^{-1}), and free energies (kJ mol^{-1}) for the ^{3}C–O activation of MTHF over a $Pd_2P(001)$ surface (523 K). These states correspond to the reaction coordinate diagram in Figure 6d.

		$C_5H_{10}O \rightarrow C_5H_9O$			$C_5H_9O \rightarrow C_5H_9O$			$C_5H_{10}O \rightarrow C_5H_{10}O$		
Rxn Coord.	BS[a]	R	TS	P	R	TS	P	R	TS	P
ΔH	0	15	176	98	91	214	87	21	223	84
ΔS	0	−175	−181	−193	−120	−110	−102	−129	−185	−178
ΔG	0	106	271	199	153	272	140	89	320	177
Figure	3n	S13p	S13q	S13r	S13s	S13t	S13u	S13v	S13w	S13x

[a]Overall values for the bare surface (BS)

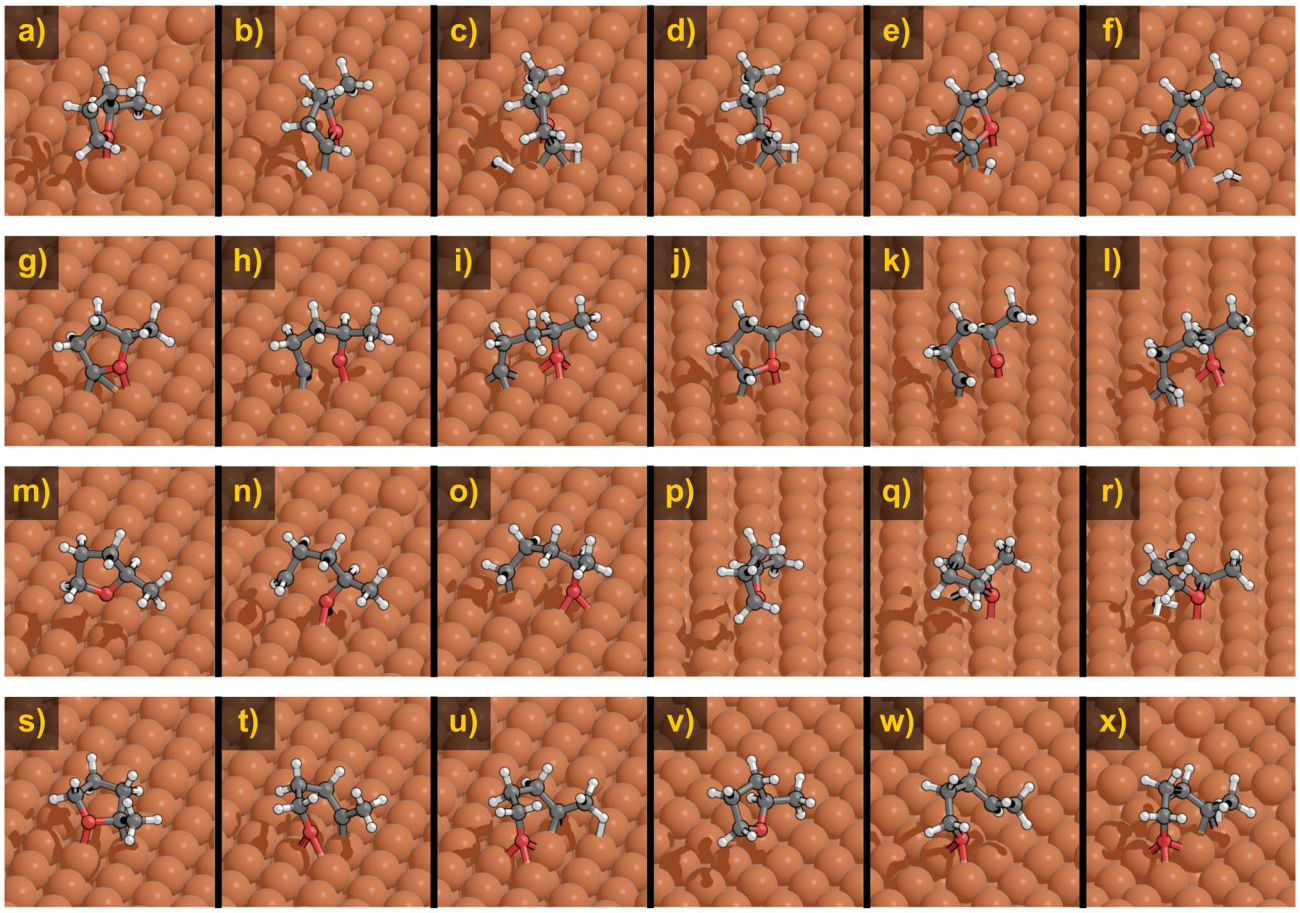

Figure S14. Structural images for the complete pathways for both the ^{2}C–O (a−i) and ^{3}C–O (p−u) activations along with the alternate C–O activations (j−o, v−x) over a Fe(0001) surface.

Table S13. Enthalpies (kJ mol^{-1}), entropies (J mol^{-1}), and free energies (kJ mol^{-1}) for the ^{2}C–O activation of MTHF over a Fe(0001) surface (523 K). These states correspond to the reaction coordinate diagram in Figure S3a.

		$C_5H_{10}O \rightarrow C_5H_9O$			$C_5H_9O \rightarrow C_5H_8O$			$C_5H_8O \rightarrow C_5H_8O$			$C_5H_9O \rightarrow C_5H_9O$			$C_5H_{10}O \rightarrow C_5H_{10}O$		
Rxn Step	BS[a]	R	TS	P	R	TS	P	R	TS	P	R	TS	P	R	TS	P
ΔH	0	−15	53	−24	15	37	−4	23	64	−74	32	112	−72	5	95	−40
ΔS	0	−174	−212	−214	−142	−143	−127	−87	−105	−59	−166	−137	−153	−147	−209	−199
ΔG	0	76	164	88	90	112	63	68	119	−43	119	183	8	81	205	64
Figure	N/A	S14a	S14b	S14c	S14d	S14e	S14f	S14g	S14h	S14i	S14j	S14k	S14l	S14m	S14n	S14o

[a]Overall values for the bare surface (BS)

Table S14. Enthalpies (kJ mol^{-1}), entropies (J mol^{-1}), and free energies (kJ mol^{-1}) for the ^{3}C–O activation of MTHF over a Fe(0001) surface (523 K). These states correspond to the reaction coordinate diagram in Figure S3b.

		$C_5H_{10}O \rightarrow C_5H_9O$			$C_5H_9O \rightarrow C_5H_9O$			$C_5H_{10}O \rightarrow C_5H_{10}O$		
Rxn Coord.	BS[a]	R	TS	P	R	TS	P	R	TS	P
ΔH	0	107	94	25	76	127	15	−6	99	−28
ΔS	0	−183	−202	−210	−143	−117	−147	−211	−206	−213
ΔG	0	202	199	135	150	188	91	104	207	84
Figure	N/A	S14p	S14q	S14r	S14s	S14t	S14u	S14v	S14w	S14x

[a]Overall values for the bare surface (BS)

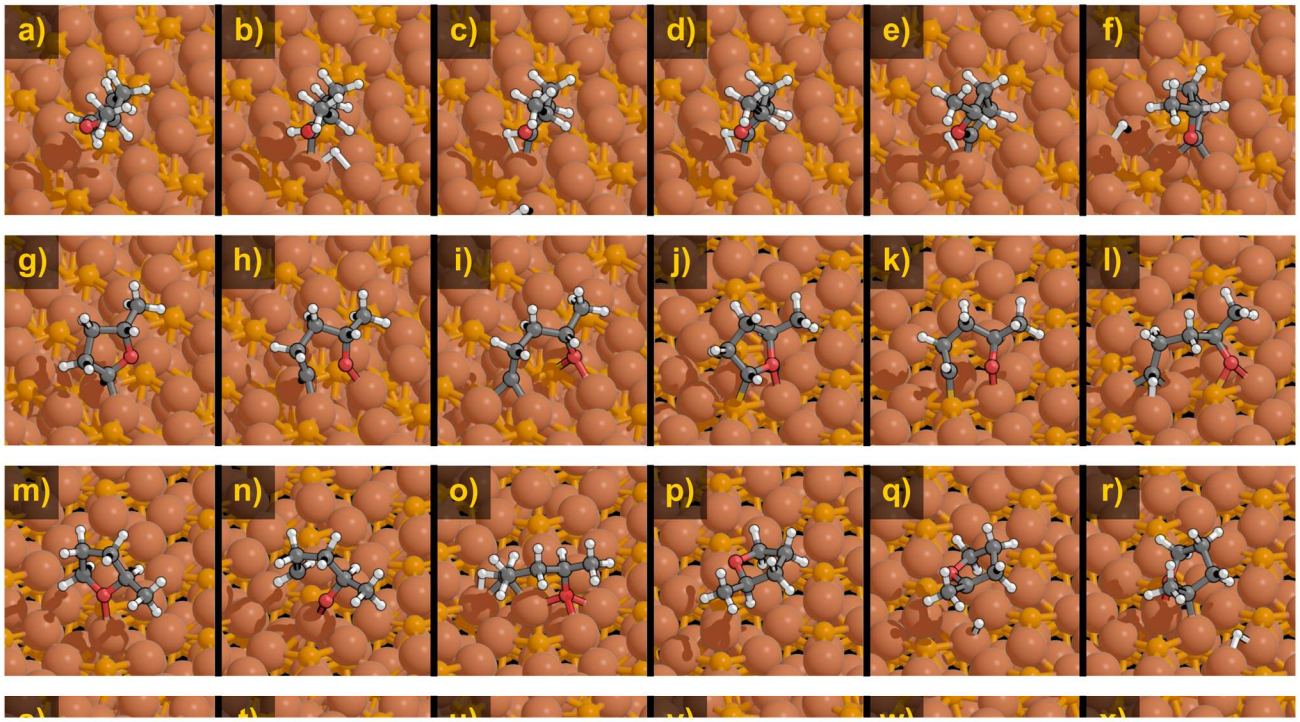

Figure S15. Structural images for the complete pathways for both the ^{2}C–O (a−i) and ^{3}C–O (p−u) activations along with the alternate C–O activations (j−o, v−x) over a $Fe_2P(001)$ surface.

Table S15. Enthalpies (kJ mol^{-1}), entropies (J mol^{-1}), and free energies (kJ mol^{-1}) for the ^{2}C–O activation of MTHF over a $Fe_2P(001)$ surface (523 K). These states correspond to the reaction coordinate diagram in Figure S3c.

		$C_5H_{10}O \rightarrow C_5H_9O$			$C_5H_9O \rightarrow C_5H_8O$			$C_5H_8O \rightarrow C_5H_8O$			$C_5H_9O \rightarrow C_5H_9O$			$C_5H_{10}O \rightarrow C_5H_{10}O$		
Rxn Step	BS[a]	R	TS	P	R	TS	P	R	TS	P	R	TS	P	R	TS	P
ΔH	0	−28	1	−68	3	9	−77	−30	15	−78	70	141	−54	−35	109	−562
ΔS	0	−196	−192	−186	−156	−140	−142	−82	−72	−63	−118	−133	−136	−202	−177	−415
ΔG	0	74	101	29	85	82	−3	12	53	−46	132	211	17	71	202	−345
Figure	3d	S15a	S15b	S15c	S15d	S15e	S15f	S15g	S15h	S15i	S15j	S15k	S15l	S15m	S15n	S15o

[a]Overall values for the bare surface (BS)

Table S16. Enthalpies (kJ mol^{-1}), entropies (J mol^{-1}), and free energies (kJ mol^{-1}) for the ^{3}C–O activation of MTHF over a $Fe_2P(001)$ surface (523 K). These states correspond to the reaction coordinate diagram in Figure S3d.

		$C_5H_{10}O \rightarrow C_5H_9O$			$C_5H_9O \rightarrow C_5H_9O$			$C_5H_{10}O \rightarrow C_5H_{10}O$		
Rxn Coord.	BS[a]	R	TS	P	R	TS	P	R	TS	P

ΔH	0	11	44	−36	−20	25	−104	−34	103	−19
ΔS	0	−179	−205	−189	−130	−153	−139	−234	−204	−173
ΔG	0	104	151	63	48	105	−32	88	210	72
Figure	3d	S15p	S15q	S15r	S15s	S15t	S15u	S15v	S15w	S15x

[a]Overall values for the bare surface (BS)

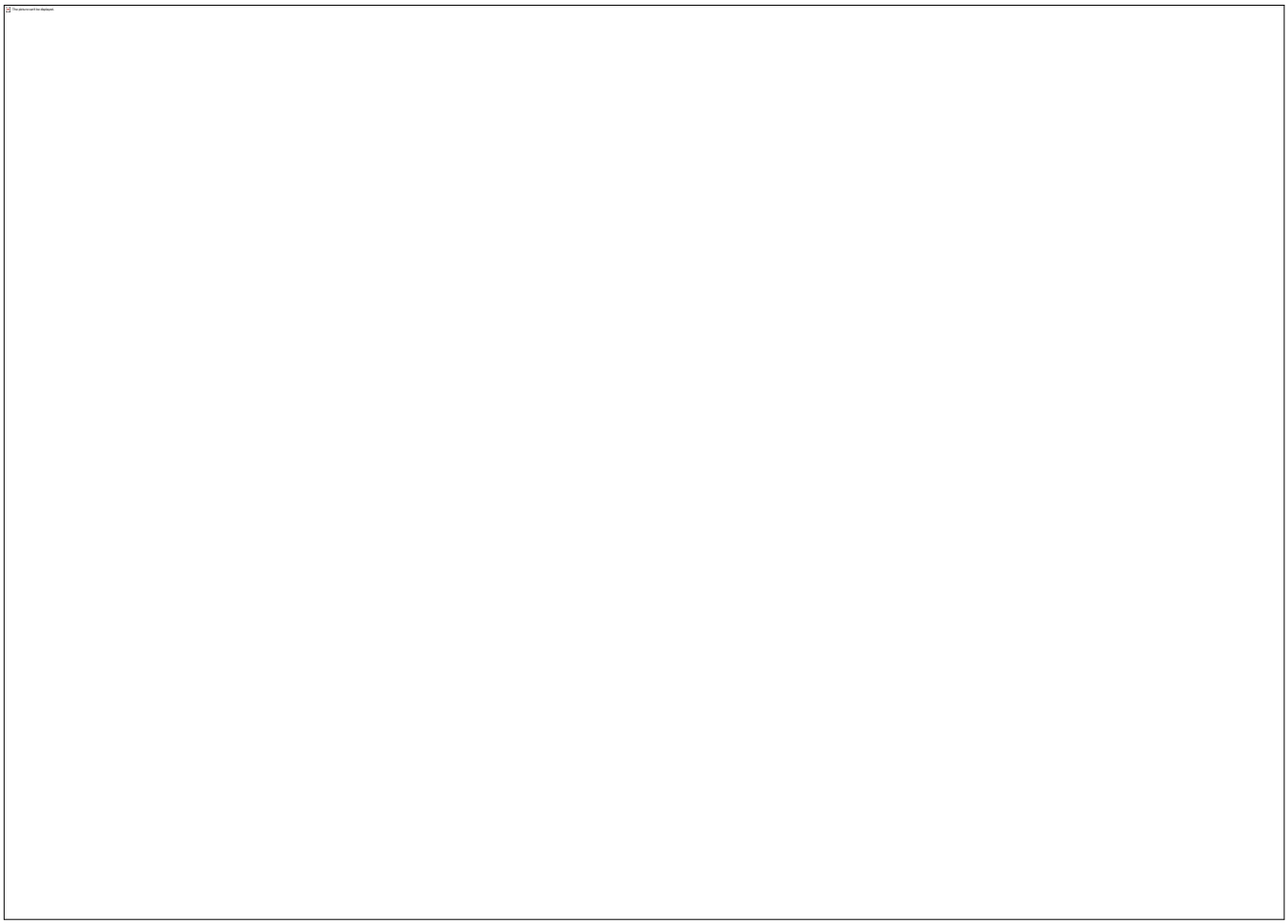

Figure S16. Structural images for both the ^{2}C–O (a−i) and ^{3}C–O (p−u) activations along with the alternate C–O activations (j−o, v−x) over a Rh(111) surface.

Table S17. Enthalpies (kJ mol^{-1}), entropies (J mol^{-1}), and free energies (kJ mol^{-1}) for the ^{2}C–O activation of MTHF over a Rh(111) surface (523 K). These states correspond to the reaction coordinate diagram in Figure S4a.

		$C_5H_{10}O \rightarrow C_5H_9O$			$C_5H_9O \rightarrow C_5H_8O$			$C_5H_8O \rightarrow C_5H_8O$			$C_5H_9O \rightarrow C_5H_9O$			$C_5H_{10}O \rightarrow C_5H_{10}O$		
Rxn Step	BS[a]	R	TS	P	R	TS	P	R	TS	P	R	TS	P	R	TS	P
ΔH	0	1	66	11	31	79	−5	34	96	4	31	111	48	−8	161	26
ΔS	0	−220	−191	−208	−138	−124	−139	−79	−61	−66	−141	−151	−123	−245	−220	−203
ΔG	0	116	166	120	103	144	68	76	128	39	105	189	112	120	276	132

Figure	N/A	S16a	S16b	S16c	S16d	S16e	S16f	S16g	S16h	S16i	S16j	S16k	S16l	S16m	S16n	S16o

[a]Overall values for the bare surface (BS)

Table S18. Enthalpies (kJ mol^{-1}), entropies (J mol^{-1}), and free energies (kJ mol^{-1}) for the ^{3}C–O activation of MTHF over a Rh(111) surface (523 K). These states correspond to the reaction coordinate diagram in Figure S4b.

		$C_5H_{10}O \rightarrow C_5H_9O$			$C_5H_9O \rightarrow C_5H_9O$			$C_5H_{10}O \rightarrow C_5H_{10}O$		
Rxn Coord.	BS[a]	R	TS	P	R	TS	P	R	TS	P
ΔH	0	0	99	45	59	129	86	−5	165	78
ΔS	0	−223	−190	−180	−144	−137	−151	−219	−167	−201
ΔG	0	116	198	139	134	201	165	110	252	183
Figure	N/A	S16p	S16q	S16r	S16s	S16t	S16u	S16v	S16w	S16x

[a]Overall values for the bare surface (BS)

Figure S17. Structural images for the complete pathways for both the ^{2}C–O (a−i) and ^{3}C–O (p−u) activations along with the alternate C–O activations (j−o, v−x) over a $Rh_2P(001)$ surface.

Table S19. Enthalpies (kJ mol^{-1}), entropies (J mol^{-1}), and free energies (kJ mol^{-1}) for the ^{2}C–O activation of MTHF over a $Rh_2P(001)$ surface (523 K). These states correspond to the reaction coordinate diagram in Figure S4c.

		$C_5H_{10}O \rightarrow C_5H_9O$			$C_5H_9O \rightarrow C_5H_8O$			$C_5H_8O \rightarrow C_5H_8O$			$C_5H_9O \rightarrow C_5H_9O$			$C_5H_{10}O \rightarrow C_5H_{10}O$		
Rxn Step	BS[a]	R	TS	P	R	TS	P	R	TS	P	R	TS	P	R	TS	P
ΔH	0	43	106	60	89	112	42	80	185	119	92	171	58	49	184	55
ΔS	0	−236	−196	−187	−153	−133	−110	−77	−64	−90	−153	−123	−132	−210	−179	−181
ΔG	0	167	209	158	169	182	100	120	219	166	172	235	127	159	278	149
Figure	3j	S17a	S17b	S17c	S17d	S17e	S17f	S17g	S17h	S17i	S17j	S17k	S17l	S17m	S17n	S17o

[a]Overall values for the bare surface (BS)

Table S20. Enthalpies (kJ mol^{-1}), entropies (J mol^{-1}), and free energies (kJ mol^{-1}) for the ^{3}C–O activation of MTHF over a $Rh_2P(001)$ surface (523 K). These states correspond to the reaction coordinate diagram in Figure S4d.

		$C_5H_{10}O \rightarrow C_5H_9O$			$C_5H_9O \rightarrow C_5H_9O$			$C_5H_{10}O \rightarrow C_5H_{10}O$		
Rxn Coord.	BS[a]	R	TS	P	R	TS	P	R	TS	P
ΔH	0	48	134	88	106	196	82	−386	190	−372
ΔS	0	−186	−180	−164	−137	−125	−132	−415	−210	−415
ΔG	0	146	228	174	178	262	151	−169	300	−155
Figure	3j	S17p	S17q	S17r	S17s	S17t	S17u	S17v	S17w	S17x

[a]Overall values for the bare surface (BS)

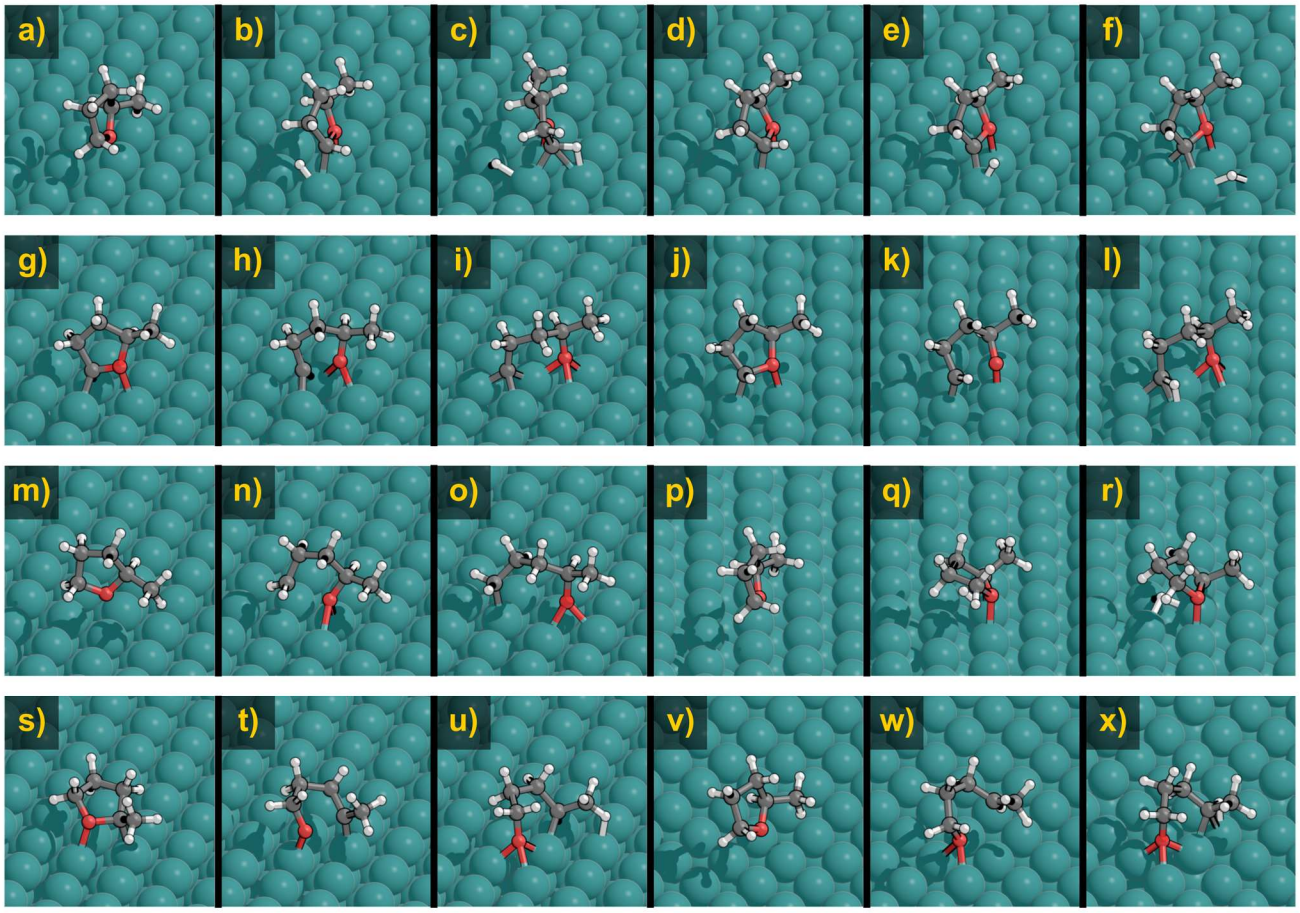

Figure S18. Structural images for the complete pathways for both the ^{2}C–O (a–i) and ^{3}C–O (p–u) activations along with the alternate C–O activations (j–o, v–x) over a Ru(0001) surface.

Table S21. Enthalpies (kJ mol^{-1}), entropies (J mol^{-1}), and free energies (kJ mol^{-1}) for the ^{2}C–O activation of MTHF over a Ru(0001) surface (523 K). These states correspond to the reaction coordinate diagram in Figure S5a.

		$C_5H_{10}O \rightarrow C_5H_9O$			$C_5H_9O \rightarrow C_5H_8O$			$C_5H_8O \rightarrow C_5H_8O$			$C_5H_9O \rightarrow C_5H_9O$			$C_5H_{10}O \rightarrow C_5H_{10}O$		
Rxn Step	BS[a]	R	TS	P	R	TS	P	R	TS	P	R	TS	P	R	TS	P
ΔH	0	−9	55	−13	29	56	−9	41	95	−64	29	73	−35	−1	138	−9
ΔS	0	−249	−200	−213	−139	−134	−143	−76	−86	−70	−142	−148	−128	−214	−208	−192
ΔG	0	121	159	98	101	126	66	81	140	−27	103	151	32	111	247	92
Figure	N/A	S18a	S18b	S18c	S18d	S18e	S18f	S18g	S18h	S18i	S18j	S18k	S18l	S18m	S18n	S18o

[a]Overall values for the bare surface (BS)

Table S22. Enthalpies (kJ mol^{-1}), entropies (J mol^{-1}), and free energies (kJ mol^{-1}) for the ^{3}C–O activation of MTHF over a Ru(0001) surface (523 K). These states correspond to the reaction coordinate diagram in Figure S5b.

		$C_5H_{10}O \rightarrow C_5H_9O$			$C_5H_9O \rightarrow C_5H_9O$			$C_5H_{10}O \rightarrow C_5H_{10}O$		
Rxn Coord.	BS[a]	R	TS	P	R	TS	P	R	TS	P

ΔH	0	−5	95	44	67	111	41	−11	131	12
ΔS	0	−214	−206	−191	−122	−148	−126	−244	−207	−190
ΔG	0	107	203	143	131	188	107	116	239	111
Figure	N/A	S18p	S18q	S18r	S18s	S18t	S18u	S18v	S18w	S18x

[a]Overall values for the bare surface (BS)

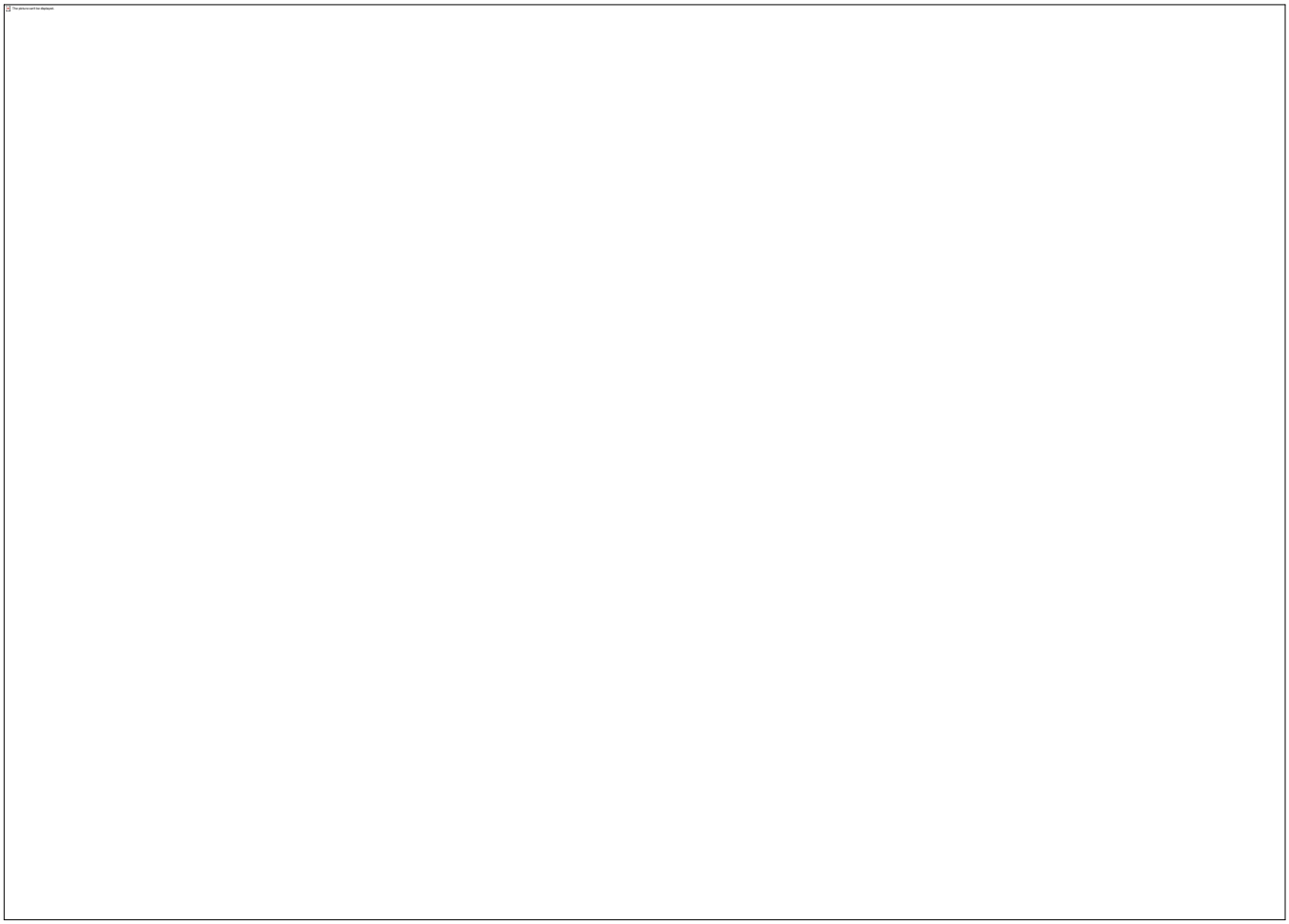

Figure S19. Structural images for the complete pathways for both the ^{2}C–O (a−i) and ^{3}C–O (p−u) activations along with the alternate C–O activations (j−o, v−x) over a $Ru_2P(001)$ surface.

Table S23. Enthalpies (kJ mol^{-1}), entropies (J mol^{-1}), and free energies (kJ mol^{-1}) for the ^{2}C–O activation of MTHF over a $Ru_2P(001)$ surface (523 K). These states correspond to the reaction coordinate diagram in Figure S5c.

		$C_5H_{10}O \rightarrow C_5H_9O$			$C_5H_9O \rightarrow C_5H_8O$			$C_5H_8O \rightarrow C_5H_8O$			$C_5H_9O \rightarrow C_5H_9O$			$C_5H_{10}O \rightarrow C_5H_{10}O$		
Rxn Step	BS[a]	R	TS	P	R	TS	P	R	TS	P	R	TS	P	R	TS	P
ΔH	0	−14	19	−37	4	13	−79	−12	28	−34	78	162	77	−24	107	−91
ΔS	0	−212	−188	−218	−148	−139	−140	−52	−75	−61	−122	−158	−133	−200	−220	−189
ΔG	0	97	117	77	82	85	−6	15	67	−2	142	245	147	81	222	8
Figure	3h	S19a	S19b	S19c	S19d	S19e	S19f	S19g	S19h	S19i	S19j	S19k	S19l	S19m	S19o	S19p

[a]Overall values for the bare surface (BS)

Table S24. Enthalpies (kJ mol^{-1}), entropies (J mol^{-1}), and free energies (kJ mol^{-1}) for the ^{3}C–O activation of MTHF over a $Ru_2P(001)$ surface (523 K). These states correspond to the reaction coordinate diagram in Figure S5d.

		$C_5H_{10}O \rightarrow C_5H_9O$			$C_5H_9O \rightarrow C_5H_9O$			$C_5H_{10}O \rightarrow C_5H_{10}O$		
Rxn Coord.	BS[a]	R	TS	P	R	TS	P	R	TS	P
ΔH	0	−20	37	−36	20	93	−59	−456	49	−420
ΔS	0	−212	−167	−189	−153	−123	−134	−415	−211	−415
ΔG	0	90	125	63	100	157	11	−239	159	−203
Figure	3h	S19p	S19q	S19r	S19s	S19t	S19u	S19v	S19w	S19x

[a]Overall values for the bare surface (BS)

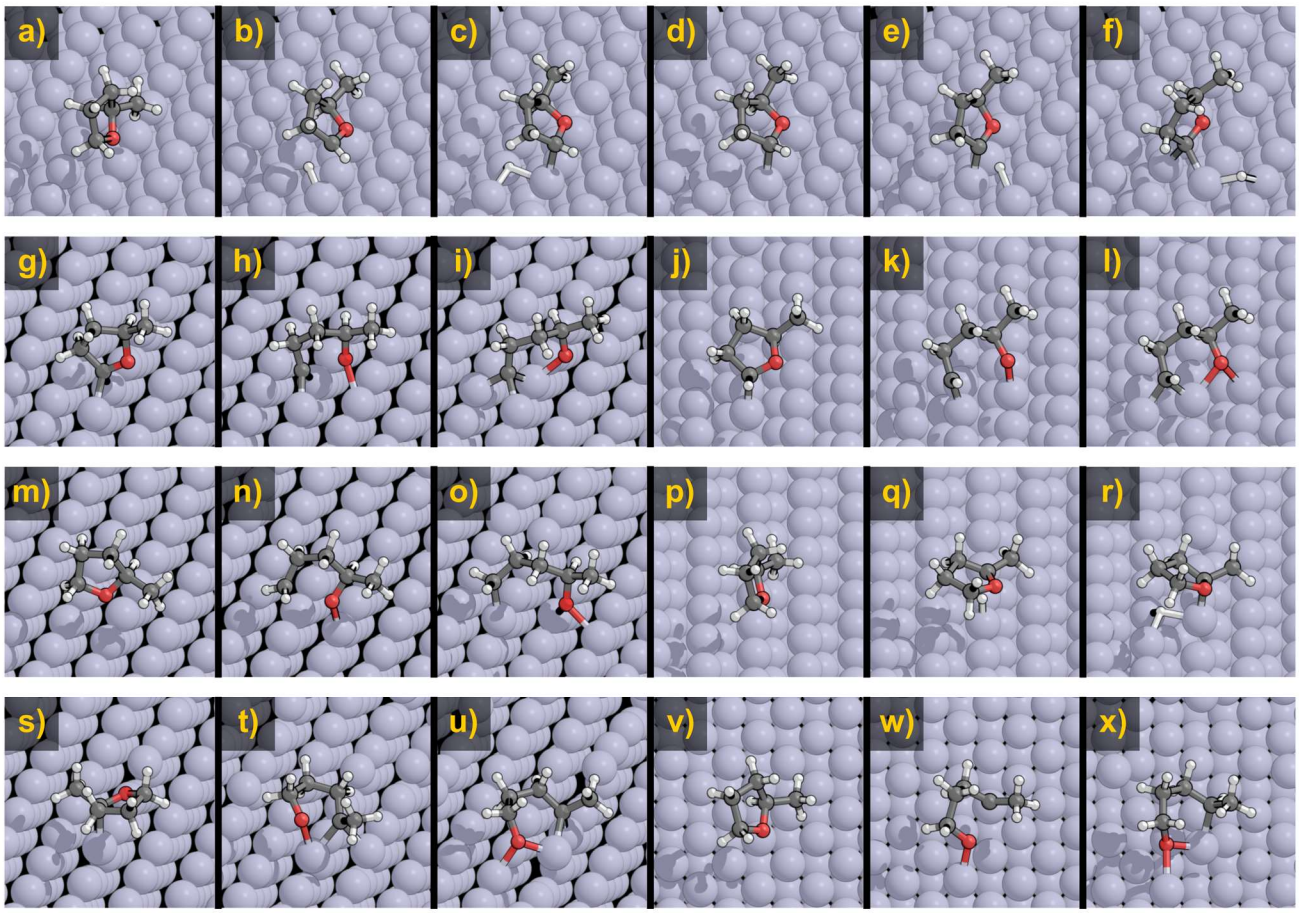

Figure S20. Structural images for the complete pathways for both the ^{2}C–O (a−i) and ^{3}C–O (p−u) activations along with the alternate C–O activations (j−o, v−x) over a Pt(111) surface.

Table S25. Enthalpies (kJ mol^{-1}), entropies (J mol^{-1}), and free energies (kJ mol^{-1}) for the ^{2}C–O activation of MTHF over a Pt(111) surface (523 K). These states correspond to the reaction coordinate diagram in Figure S6a.

		$C_5H_{10}O \rightarrow C_5H_9O$			$C_5H_9O \rightarrow C_5H_8O$			$C_5H_8O \rightarrow C_5H_8O$			$C_5H_9O \rightarrow C_5H_9O$			$C_5H_{10}O \rightarrow C_5H_{10}O$		
Rxn Step	BS[a]	R	TS	P	R	TS	P	R	TS	P	R	TS	P	R	TS	P
ΔH	0	−3	69	7	14	92	0	24	173	115	18	163	128	−6	197	105
ΔS	0	−189	−208	−152	−126	−111	−108	−82	−86	−85	−97	−115	−131	−241	−162	−205
ΔG	0	96	178	86	80	150	57	67	218	160	69	223	197	120	281	212
Figure	N/A	S20a	S20b	S20c	S20d	S20e	S20f	S20g	S20h	S20i	S20j	S20k	S20l	S20m	S20o	S20p

[a]Overall values for the bare surface (BS)

Table S26. Enthalpies (kJ mol^{-1}), entropies (J mol^{-1}), and free energies (kJ mol^{-1}) for the ^{3}C–O activation of MTHF over a Pt(111) surface (523 K). These states correspond to the reaction coordinate diagram in Figure S6b.

		$C_5H_{10}O \rightarrow C_5H_9O$			$C_5H_9O \rightarrow C_5H_9O$			$C_5H_{10}O \rightarrow C_5H_{10}O$		
Rxn Coord.	BS[a]	R	TS	P	R	TS	P	R	TS	P
ΔH	0	−9	49	31	−352	223	168	−11	170	148
ΔS	0	−243	−180	−200	−341	−151	−135	−239	−167	−200
ΔG	0	118	144	136	−173	302	239	114	257	252
Figure	N/A	S20p	S20q	S20r	S20s	S20t	S20u	S20v	S20w	S20x

[a]Overall values for the bare surface (BS)

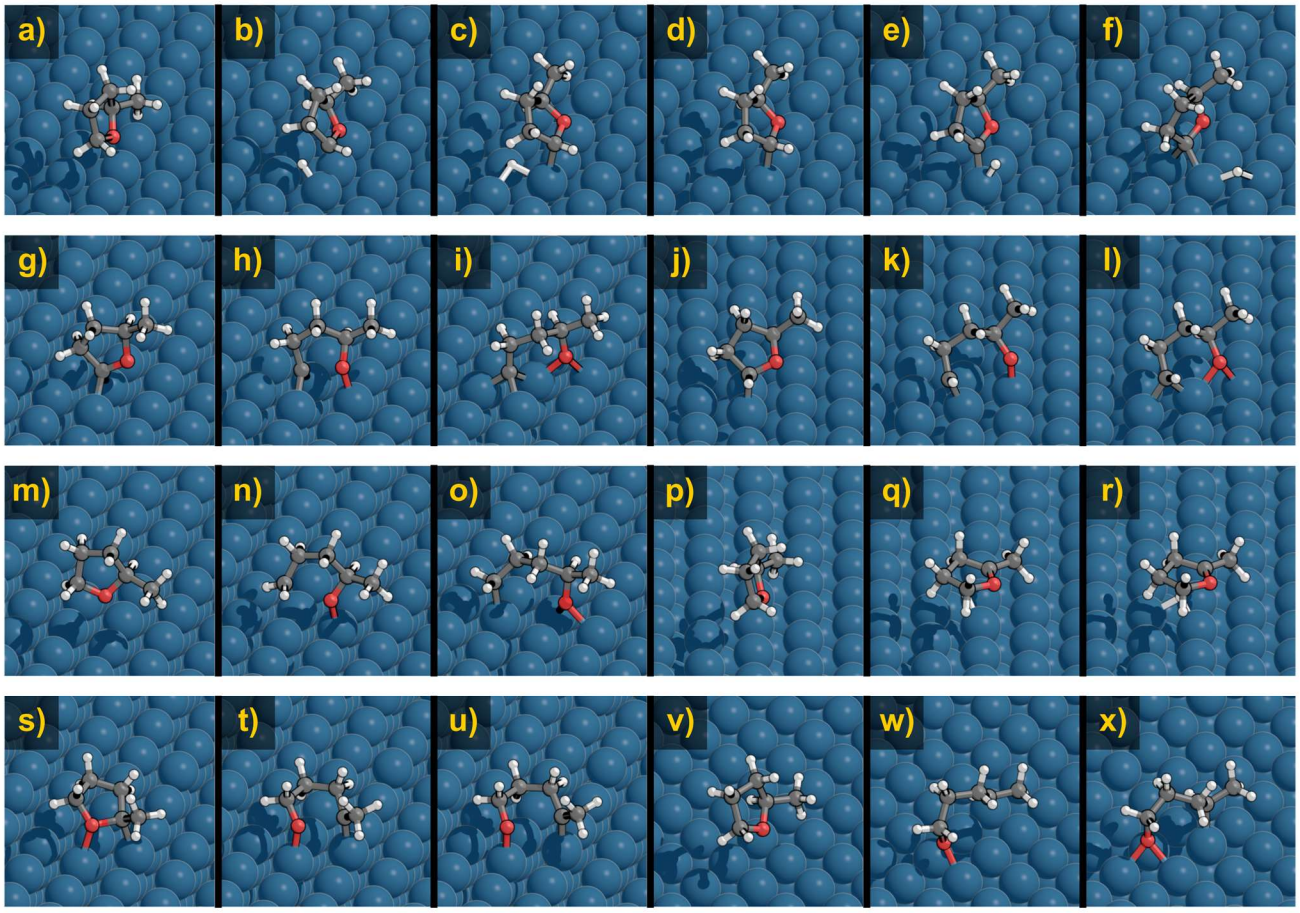

Figure S21. Structural images for the complete pathways for both the ^{2}C–O (a–i) and ^{3}C–O (p–u) activations along with the alternate C–O activations (j–o, v–x) over a Ir(111) surface.

Table S27. Enthalpies (kJ mol^{-1}), entropies (J mol^{-1}), and free energies (kJ mol^{-1}) for the ^{2}C–O activation of MTHF over a Ir(111) surface (523 K). These states correspond to the reaction coordinate diagram in Figure S7a.

		$C_5H_{10}O \rightarrow C_5H_9O$			$C_5H_9O \rightarrow C_5H_8O$			$C_5H_8O \rightarrow C_5H_8O$			$C_5H_9O \rightarrow C_5H_9O$			$C_5H_{10}O \rightarrow C_5H_{10}O$		
Rxn Step	BS[a]	R	TS	P	R	TS	P	R	TS	P	R	TS	P	R	TS	P
ΔH	0	−11	86	29	38	83	10	40	100	50	40	127	85	−11	176	75
ΔS	0	−231	−217	−219	−158	−158	−163	−75	−68	−90	−153	−133	−135	−240	−223	−176
ΔG	0	110	199	144	121	166	95	79	136	97	120	197	155	115	292	168
Figure	N/A	S21a	S21b	S21c	S21d	S21e	S21f	S21g	S21h	S21i	S21j	S21k	S21l	S21m	S21o	S21p

[a]Overall values for the bare surface (BS)

Table S28. Enthalpies (kJ mol^{-1}), entropies (J mol^{-1}), and free energies (kJ mol^{-1}) for the ^{3}C–O activation of MTHF over a Ir(111) surface (523 K). These states correspond to the reaction coordinate diagram in Figure S7b.

		$C_5H_{10}O \rightarrow C_5H_9O$			$C_5H_9O \rightarrow C_5H_9O$			$C_5H_{10}O \rightarrow C_5H_{10}O$		
Rxn Coord.	BS[a]	R	TS	P	R	TS	P	R	TS	P

ΔH	0	−2	62	54	72	107	109	−9	187	104
ΔS	0	−206	−192	−196	−149	−140	−114	−242	−210	−205
ΔG	0	106	163	156	150	181	168	117	297	212
Figure	N/A	S21p	S21q	S21r	S21s	S21t	S21u	S21v	S21w	S21x

[a]Overall values for the bare surface (BS)

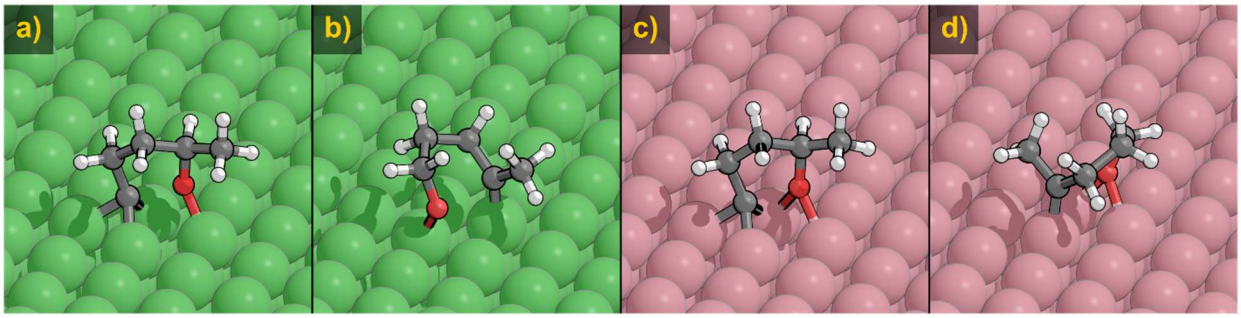

ΔH≠	125	172	123	159
ΔS≠	–77	–137	–77	–132
ΔG≠	166	244	163	228

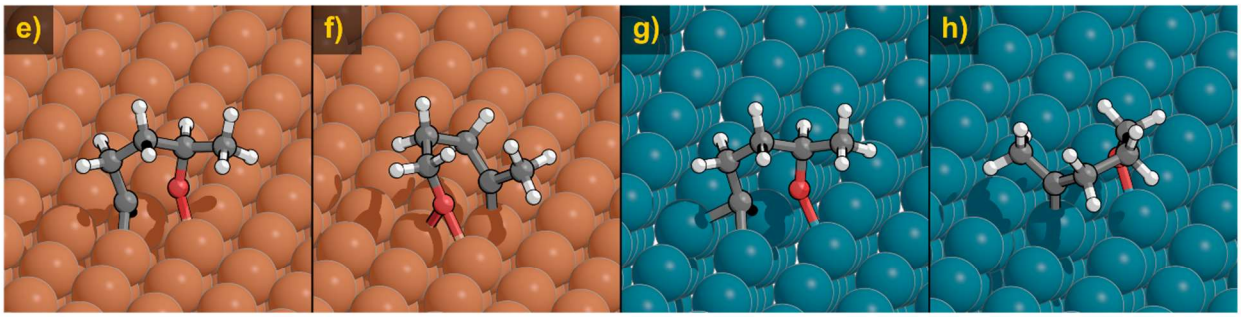

ΔH≠	64	127	168	216
ΔS≠	–105	–117	–78	–151
ΔG≠	119	188	209	295

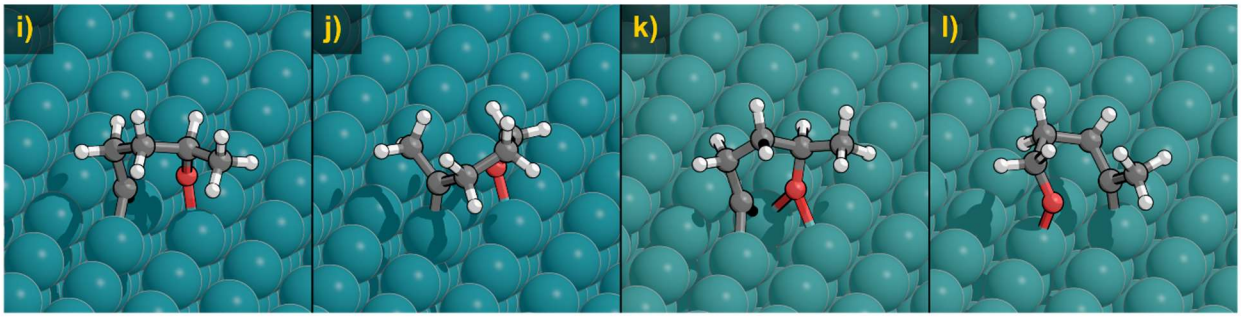

ΔH≠	96	129	95	111
ΔS≠	–61	–137	–86	–148
ΔG≠	128	201	140	188

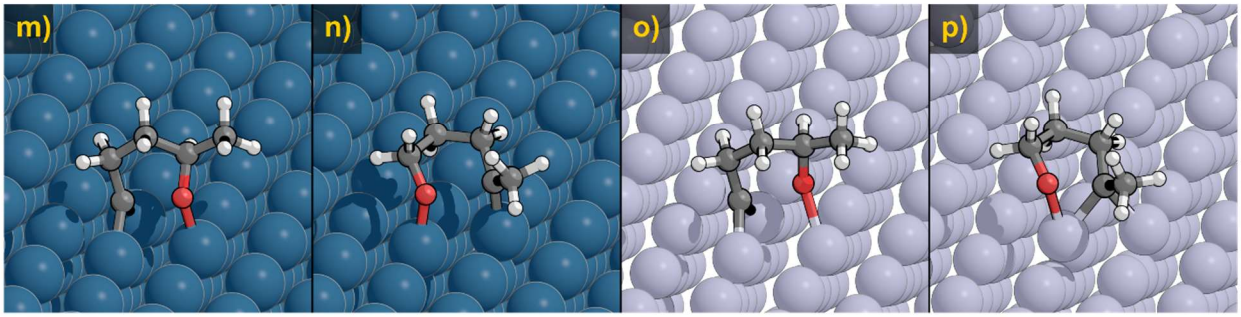

ΔH≠	100	107	173	223
ΔS≠	–68	–140	–86	–151
ΔG≠	136	181	218	302

Figure S22. The transition states for the unhindered C–O bond (^{2}C–O) activation (a,c,e,g,i,k,m,o) and the hindered C–O bond (^{3}C–O) activation (b,d,f,h,j,l,n,p) on all of the pure metal surfaces investigated. Underneath are the ΔH (kJ mol^{-1}), ΔS (J mol^{-1}), and ΔG (kJ mol^{-1}) values for each transition state.

S5. *Periodic Trends*

There are observed periodic trends with fully dehydrogenated C–O activation barriers and with the ΔΔH values that potentially indicate opposite trends in selectivity and activity. The Group 10 (right side) metals have the larger enthalpy barriers and, in general, a similar trend can be seen going down the columns with the elements in the bottom typically having the largest activation enthalpy for their group (Figure S22). Ni_2P and Pd_2P (Group 10) are selective towards ^{3}C–O activation (positive $\Delta\Delta H_{act}$) (Figure 8). These phosphides, however, have high activation barriers compared to the other metals. On the other hand, Fe_2P and Ru_2P had relatively poor selectivity for ^{3}C–O activation, especially since Ru_2P showed a decrease in ΔΔH values with the addition of P in comparison to Ru. These two materials, however, have the lowest enthalpy barriers of the metals. These trends match those described for $\Delta G^{\ddagger}$ (Figure 9). These trends potentially indicate high selectivity with low activity for Ni and Pd, while metals like Fe and Ru have higher activity and worse selectivity. Activation barriers, however, are not an adequate descriptor for activity as they do not account for coverage effects which can strongly affect reaction rates. The trends in the ΔΔH values for the pure metal surfaces showed only a very weak trend of having the Group 10 metals (i.e. Ni, Pd, and Pt) be the least favorable for ^{3}C–O activation (Figure S23). This trend flips and is more pronounced in the phosphide materials with Ni_2P and Pd_2P (Section 3.1 and 3.3) being the most favorable for ^{3}C–O activation. Again, these trends match those seen for ΔΔG (Figure 10). These trends suggest that the valence shells and other electronic properties of the metals may also play a role in shifting the selectivity.

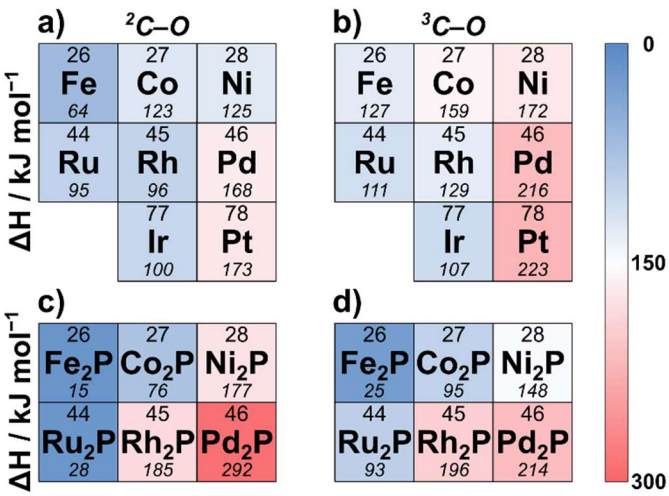

Figure S23. Periodic table trends for the fully dehydrogenated free energy barriers (ΔH_{act}, kJ mol^{-1}) for the ^{2}C–O activation for pure metal (a) and M_2P (c) surfaces and ^{3}C–O activation for pure metal (b) and M_2P (d) surfaces. Red coloring indicates high ΔH_{act} values and blue indicates low ΔH_{act} values.

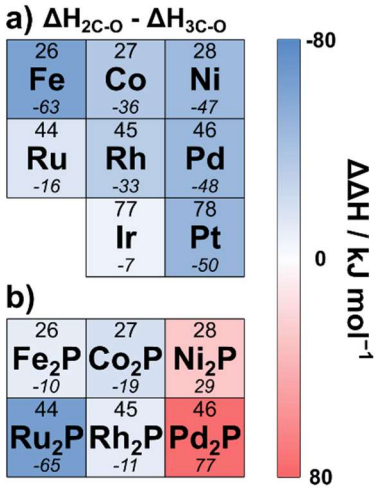

Figure S24. Periodic table trends for the difference in fully dehydrogenated free energy barriers (ΔΔH, kJ mol^{-1}) relative to the bare surface for the pure metals (a) and the M_2P surfaces (b). Red indicates the most selective towards ^{3}C–O activation and blue indicates the most selective towards ^{2}C–O activation.